AN ABSTRACT OF THE THESIS OF

BRUCE HUEHN for the degree of MASTER OF SCIENCE

in GEOPHYSICS presented on _____

Title: CRUSTAL STRUCTURE OF THE BAJA PENINSULA BETWEEN LATITUDES 22°N and 25°N

Abstract approved: Redacted for Privacy

Richard W. Couch

Geophysical data collected in 1975 and 1976 reveal major crustal and tectonic elements of the continental margin of southern Baja California. Gravity, magnetic, seismic reflection and bathymetric data show seaward extension of the islands enclosing Magdalena and Almejas Bays. A seismic reflection profile, oriented approximately normal to the trend of the Baja peninsula, indicates normal faulting of the near surface sediment layers along the outer continental shelf. The reflection record also shows that sediment layers immediately above the acoustic basement dip toward the east at the base of the continental slope. A crustal and subcrustal cross section, oriented approximately parallel to the reflection profile and constrained by gravity, magnetic, bathymetric and seismic refraction data, indicates a maximum crustal thickness of approximately 21 km for Baja California, making it intermediate in thickness between normal continental and normal oceanic crusts. The section also

indicates a low density zone in the mantle below the Gulf of California. Magnetic anomalies along the cross section require oceanic crust of the Pacific Plate to extend at least 50 km landward of the edge of the western continental shelf of Baja California. This suggests either a past period of oblique subduction of the Pacific Plate beneath Baja California or emplacement of Pacific Plate oceanic crust beneath the peninsula by descending spreading centers of the East Pacific Rise.

Crustal Structure of the Baja Peninsula between Latitudes 22°N and 25°N

by

Bruce Huehn

A THESIS

submitted to

Oregon State University

in partial fulfillment of
the requirements for the
degree of

Master of Science

Commencement June 1977

APPROVED:

Redacted for Privacy

Associate Professor of Geophysics
in charge of major

Redacted for Privacy

Dean of School of Oceanography

Redacted for Privacy

Dean of Graduate School

Date thesis is presented 28 April 1977

Typed by Mary Jo Stratton for Bruce Huehn

ACKNOWLEDGEMENTS

Special thanks go to Dr. Richard Couch who served as my advisor while I was a graduate student. His help and criticism were indispensable in the preparation of my thesis.

Michael Gemperle and Gerald Connard provided assistance in matters concerning the measurement and reduction of gravity and magnetic data. Virginia Taylor and Barbara Priest drafted the figures that appear in this thesis.

Conversations with fellow students, Shane Coperude, Paul Jones, Keith Wrolstad, Tom Plawman and Gustavo Calderon Riveroll, were both enlightening and enjoyable.

Shannon Huehn is hereby recognized for typing and proof-reading preliminary manuscripts. I am grateful for her help and moral support.

This work was conducted with the support and cooperation of the Direccion General de Oceanografia, Mexico and was supported in part by the Office of Naval Research through contract number N00014-76-C-0067, under project NR 083-102.

TABLE OF CONTENTS

LIST OF TABLES

LIST OF FIGURES

CRUSTAL STRUCTURE OF THE BAJA PENINSULA BETWEEN LATITUDES 22°N AND 25°N

INTRODUCTION

The Gulf of California separates the approximately 1300 km long peninsula of Baja California from mainland Mexico. The width of Baja California varies from 41 km in the south near the city of La Paz to 275 km just south of Vizcaino Bay. A rugged, mountainous terrain and a narrow shelf in the gulf characterize the peninsula's east side. The western side, however, slopes gradually toward the Pacific Ocean and has a relatively wide continental shelf and slope. The floor of the gulf is bounded on the south by the Tomayo Fracture Zone and is the point of intersection of the North American continent and the East Pacific Rise. Within the gulf, bathymetric and seismic reflection measurements have established the presence of a series of parallel faults which trend about north 55° west, approximately 20° west of the trend of the peninsula and gulf. The interpretation of marine geophysical data (e.g. Vine, 1966; Larson et al., 1968; Thatcher and Brune, 1971) has shown that these general features are associated with sea-floor spreading in the Gulf of California.

In 1975 personnel of the Direccion General de Oceanografia, Mexico, and the Oregon State University Geophysics Group initiated a joint geophysical investigation of the Gulf of California and the

Pacific Ocean off the coast of Baja California. The cruises that resulted from this program, Baja-75 and Baja-76, yielded over 23,000 km of continuous gravity, magnetic and bathymetric measurements in the gulf and along the western continental margin of Baja California. Three seismic reflection profiles and three reversed wide angle reflection and refraction lines were also obtained during Baja-76. The two groups conducted the investigation aboard the Mexican oceanographic research vessel, DM-20. The results of these two cruises, particularly Baja-75, provide the primary source of data for this paper.

This study investigates the earth's crustal and subcrustal structure in the vicinity of Baja California between latitudes 22°N and 25°N. Other than what is indicated by isolated seismic refraction stations and surface geology, very little is known about the structure. A cross section, computed to a depth of 50 km and constrained by gravimetric, seismic, magnetic, bathymetric and geologic data, models the crust and upper mantle along a profile that crosses the peninsula and Gulf of California. This study also analyzes contoured gravity and magnetic anomaly maps in terms of surface or near-surface geologic structure and compares the model cross section to previous works concerning the area's tectonic evolution (e.g., Atwater, 1970).

PREVIOUS WORK

Marine Geologic and Geophysical Studies

Menard (1960) reported that the East Pacific Rise intersects the North American continent at the mouth of the Gulf of California. Wilson (1965) and Vine (1966) propose that the intersection suggests a relationship between the gulf and ocean ridge system. Their plate tectonic models relate the origin of the gulf to sea-floor spreading at the East Pacific Rise. This hypothesis supports an older idea, i.e., that the Gulf of California was formed by the separation of Baja California from mainland Mexico.

Hamilton (1961) was the first to consider this idea in detail, although not in the context of plate tectonics. He suggested the separation of Baja California from mainland Mexico is indicated by the fact that the Gulf of California longitudinally bisects the batholithic rock belt of the North American Cordillera. Furthermore, the limited amount of geophysical data existing at that time, in the form of seismic refraction, gravity and heat flow measurements, indicated the floor of the gulf is oceanic rather than continental. This refuted the possibility that the gulf is a graben type structure resulting from the collapse of a block of continental crust.

A seismic refraction study by Phillips (1964) indicated crustal thicknesses between 7 and 13 km in the southern half of the Gulf of

California, and lower than average seismic velocities (7.6-7.9 km/sec) for the upper mantle material. The significance of these values is that, throughout the world, lower than average mantle velocities are associated with sea-floor spreading ridge systems (e.g., Shor et al., 1970). On the basis of these velocity magnitudes, Phillips (1964) concluded the southern part of the gulf has a structure similar to the East Pacific Rise.

Von Herzen's (1963) heat flow measurements supported Phillips' conclusion. Thirteen measurements near the mouth and in the Gulf of California indicated a mean of 3.17 $\mu cal/cm^2$-sec, which is substantially higher than the mean oceanic value of 1.5 $\mu cal/cm^2$-sec (Lee, 1970). Because heat flow values over mid-oceanic ridges are higher than the worldwide average (Lee, 1970), Von Herzen concluded that the observations suggest a continuation of the East Pacific Rise into the gulf.

Harrison and Mathur (1964) studied gravity anomalies in the Gulf of California and found that, south of 28^{o}N Lat., the gulf floor is characterized by large positive Bouguer anomalies which decrease to about zero mgal at the east and west coasts. The authors noted that this is typical of the gravity field over oceanic crust, and they believed the area to be in near isostatic equilibrium. This would not be the case had the gulf formed by subsidence of continental crust.

Rusnack et al. (1964) reviewed a large volume of bathymetric data from the Gulf of California and confirmed the existence of a series of en echelon faults trending approximately 20° west of the gulf axis. Based on lateral offsets in the gulf's bathymetry and the history of fault motion in southern California, the authors interpreted the faults to be a southward continuation of the right-lateral strike-slip San Andreas fault system. This interpretation quite reasonably led to their conclusion that the Baja peninsula was displaced from mainland Mexico by motion along this fault system.

Wilson (1965) suggested that the San Andreas fault acts as a dextral ridge-ridge transform fault, connecting the East Pacific Rise, at the mouth of the Gulf of California, with the Gorda and Juan de Fuca Ridges in the northeast Pacific. This implied that the gulf has opened along this single transform fault. However, Menard (1966) used bathymetric data to show that the East Pacific Rise is segmented by small fracture zones as it approaches the mouth of the gulf. Noting this relatively high frequency segmentation and using mapped faults and bathymetric data, Vine (1966) proposed the opening of the gulf originates at spreading centers offset by the series of en echelon faults described by Rusnack et al. (1964), which Wilson did not consider. Although Vine's interpretation differed from Wilson's the fundamental mechanism in both was the same. Both proposed the gulf opened along a fault or faults connecting ocean ridge segments

where sea-floor spreading occurs. This placed the separation of Baja California from mainland Mexico in the context of plate tectonics. In terms of plate tectonics, the Baja peninsula and southwest California, as part of the Pacific Plate, have moved along transform faults in a strike-slip manner with respect to the North American Plate.

Larson et al. (1968) and Moore and Buffington (1968) conducted separate magnetic surveys at the mouth of the Gulf of California. The former conducted the more extensive survey and provided a map of the magnetic anomaly lineations from just north of the Rivera Fracture Zone to just north of the Tomayo Fracture Zone. Larson et al. (1968) reported an offset of 75 km in the East Pacific Rise across the Tomayo Fracture Zone, a half spreading rate of 3.0 cm/yr, and that most of the spreading at the mouth of the Gulf of California has occurred in the last 4 million years (m.y.). The last conclusion was based on the identification of a 4 m.y. old magnetic event just off the tip of Baja California and the assumption that the peninsula has moved with the west flank of the East Pacific Rise. Moore and Buffington (1968) established a half spreading rate of 3.0 to 3.5 cm/yr and also concluded that the present cycle of spreading started 4 m.y. ago. Their latter result, however, was reached by dividing a 3.0 cm/yr half spreading rate into the distance (120 km) between the rise crest and the 1000 fathom contour off the tip of Baja California.

Atwater (1970) interpreted magnetic anomalies of the entire northeast Pacific. In the area between the southern tip of Baja California and the Mendocino Fracture Zone (40°N), no active sea-floor spreading ridge exists. Magnetic anomaly lineations show the crustal age increasing seaward of North America and no symmetry in the anomaly pattern. To account for this she concluded that a trench once existed off the coast of North America. This trench consumed the Farallon Plate, which contained the missing half of the symmetrical pattern of magnetic anomalies, and ultimately the ridge itself. From this hypothesis Atwater related the youngest identifiable anomalies, adjacent to the North American coast, to a time when the ridge was still spreading and the trench still active. For the area west of Baja California, the age of the youngest anomalies varies from 18 m.y. in the north to 6 m.y. on the west side of the southern tip.

Atwater (1970) dealt with the plate tectonic evolution of this area by considering two types of plate models, one with constant motion and the other with time dependent motion. Although the facts did not clearly support one over the other, she concluded the former was the more probable and, with this model, described the interaction of the East Pacific Rise and the trench west of North America as a migrating ridge-trench-transform triple junction. According to McKenzie and Morgan (1969), this situation resulted in a cessation of ridge spreading

and the initiation of strike-slip motion along a transform fault where the trench used to exist. If this occurred, the youngest identifiable magnetic anomalies indicate when the ridge met the trench, resulting in the total disappearance of the Farallon Plate and the beginning of the present cycle of strike-slip motion between the Pacific and North American Plates (Atwater, 1970).

Atwater's (1970) cross sections, which model the ridge-trench collision in a time sequence also required that the East Pacific Rise became inactive as a spreading center once it made contact with the trench. Although, had it not done so, the conclusions drawn about the time of the ridge-trench collision would remain the same. The spreading centers, in the latter case, would just continue to migrate under the North American Plate. The implication of Atwater's hypothesis, however, is that once the ridge and trench met, transform fault motion ensued at the intersection. This motion supposedly continued along the axis of the former trench until the new material, emplaced by the ridge, had sufficiently cooled and was no longer the crust's line of weakness. Relative plate motion then began to take place at weaker points in the crust, e.g., in the Gulf of California and along the San Andreas fault system. In the gulf this also involved the re-emergence of the East Pacific Rise and associated sea-floor spreading, as well as motion along transform faults.

Chase et al. (1970) interpreted the magnetic anomalies west of Baja California between latitudes 21°N and 27°N and described the history of the approach of the East Pacific Rise toward the North American continent. Because the spacial orientation of a particular linear magnetic anomaly describes the spacial orientation of the ridge at the time the anomaly was formed, they were able to show how the ridge was affected by the approach of the continent. They observed that while the trend of the ridge was north-south about 22 m.y. ago, it changed its orientation considerably between 22 m.y. and 13 m.y. ago. At this latter time the ridge almost paralleled the present coast of Baja California, and south of the southern tip of the peninsula it began to trend northeast toward the Gulf of California.

Within the gulf, except for the area just north of the Tomayo Fracture Zone, magnetic anomalies, produced by sea-floor spreading, have not been found. Hilde (1964) conducted the first study in this area and concluded the anomaly patterns correspond closely to underwater topography. Larson et al. (1972) were also unable to detect any coherent magnetic anomaly lineations. They suggested that relatively rapid sedimentation rates within the gulf may have prevented the new crust from acquiring any significant amount of thermal remanent magnetization.

Larson et al. (1972) compared fault trends, found in the Gulf of California, to synthetic fracture zone trends, computed from three

different positions of the Pacific-North American pole of rotation. Morgan (1968) discussed the use of rotation poles and associated angular velocities to describe the relative motion of rigid plates on the earth's surface. He established 53°N, 53°W as the position of the pole describing the relative motion of the Pacific and North American Plates. Le Pichon (1968) calculated 53°N, 47°W as the pole position, while determinations by McKenzie and Parker (1967), Chase (cited by Larson et al., 1972) and Minster et al. (1972) produced the substantially different positions of 50°N, 85°W; 52°N, 76°W and 51°N, 65°W, respectively. The comparison by Larson et al. (1972), which did not include Le Pichon's or Minster's calculated positions, led the authors to conclude that the fracture zones generated by Chase's pole position best fit the actual fault trends in the gulf.

Thatcher and Brune (1971) studied earthquake swarm sequences in the northern Gulf of California and found recorded events to be characterized by "shallow hypocentral depths, predominantly normal faulting," and located in the deep basins, thus providing additional confirmation that the gulf's deep basins are active centers of sea-floor spreading. Also, their observations of teleseismic delays revealed low upper mantle velocities and further indicated the presence of a spreading center.

Molnar's (1973) analysis of fault plane solutions in the Gulf of California showed right-lateral strike-slip to be the predominant

motion along the gulf's en echelon faults. He also indicated that earthquakes along these faults have motion oriented about 20° east of the direction of motion for earthquakes on the Rivera Fracture Zone. This finding strongly indicated the Rivera Plate, a small, triangular section of crust bounded by the North American Plate, the Rivera Fracture Zone and the East Pacific Rise, has motion relative to the North American Plate. Therefore, calculations of the relative motion between the Pacific and North American Plates, based on magnetic anomalies south of the Tomayo Fracture Zone, were no longer considered sound. Molnar cited a rate of 5.8 cm/yr based on Atwater's (1970) interpretation of two short magnetic anomaly profiles just north of the Tomayo Fracture Zone. Reichle et al. (1976) computed a range of 3.7 to 6.1 cm/yr for the average seismic slip rate along the Gulf of California since 1918. The latter study also cited Atwater and Molnar's (1973) rate of 5.5 cm/yr, based on sea-floor spreading in the Atlantic, Indian and South Pacific Oceans.

Moore (1973) presented seismic reflection profiles across the San Padro Martir and Guaymas Basins in the Gulf of California. In agreement with fault plane solutions of earthquakes originating in the gulf basins, these reflection profiles showed normal faulting along the sides and floor of the basins. Moore also discussed the need for a protogulf prior to the initiation of the present tectonic motion in the gulf. From the location of spreading centers and fracture zones and

the rate of relative plate motion, Moore identified areas of old and new crust within the gulf. One of his arguments for the protogulf was based on his interpretation that about a kilometer of sediment on the old crust was deposited prior to the present sea-floor spreading. Applying the same features and data used to generate the map of old and new crust, Moore also produced a simple reconstruction of Baja California prior to its present period of northwest motion with respect to the North American Plate. The reconstruction indicated incomplete closure of the Gulf of California and thus suggested that a protogulf may have existed.

The geological and geophysical studies summarized above, in near chronological order, outline what is known and speculated concerning the history and structure of Baja California and the Gulf of California. Heat flow, seismic, gravity, bathymetric and magnetic data have confirmed the continuation of the East Pacific Rise into the Gulf of California. Seismic reflection, earthquake hypocenters and fault plane solutions have established right-lateral strike-slip to be the predominant motion along a series of en echelon faults in the gulf. These faults approximately parallel the trend of the San Andreas fault in California. Seismic reflection and bathymetric data and investigations of earthquake swarms strongly indicate the gulf's deep basins are active spreading centers of the East Pacific Rise. These observations and those from magnetic anomaly surveys in the southern

Gulf of California have clearly established that Baja California, as part of the Pacific Plate, is moving northwest relative to the North American Plate. The rate of relative motion is probably between 5.5 and 5.8 cm/yr.

Terrestrial Geology of Southern Baja California

Baja California lies within a segment of the North American Cordillera that is bounded on the north by the Transverse Ranges of southern California (33^{o}-35^{o}N) and on the south by the trans-Mexico volcanic belt (18^{o}-22^{o}N). These boundaries are structural features whose trends interrupt that of the Cordillera (Allison, 1964). Baja California constitutes practically the entire physiographic province that Allison (1964) calls the Peninsular Range Province. A large portion of the northern half of this province, in particular its higher elevations, is exposed late Mesozoic granitic rocks of the Peninsular Range Batholith. These rocks, with ages similar to other western North American Cordillera plutons (92-115 m.y.) are largely absent from the peninsula's surface geology south of 28^{o}N but are visible at the peninsula's southern tip.

Figure 1 shows a geologic map after Lopez Ramos (1976) of Baja California in the vicinity of the study area. From 28^{o}N Lat. down to 24^{o}N Lat. the andesitic, pyroclastic and related epiclastic rocks of the Comondu Formation dominate the surface geology of Baja California.

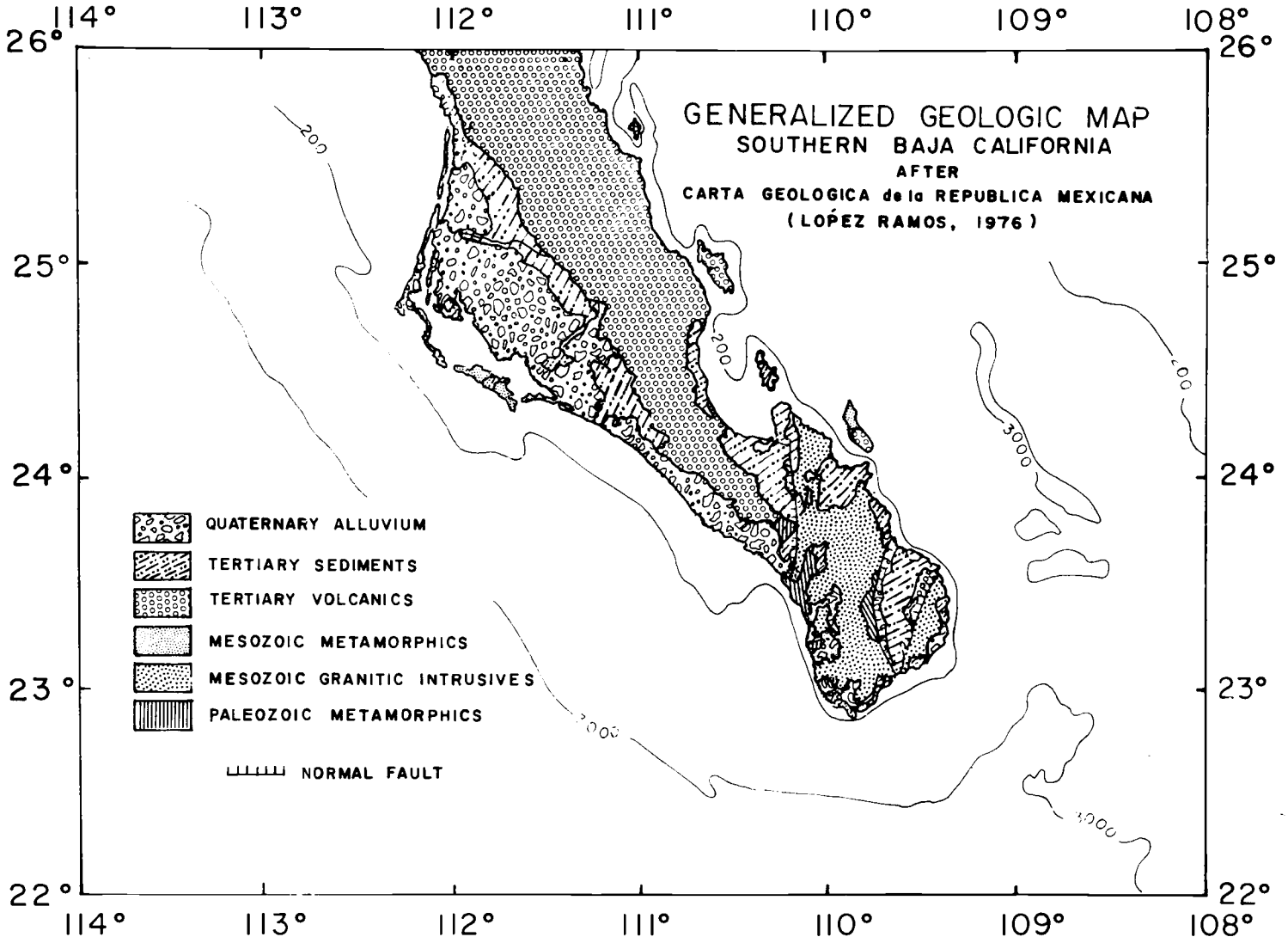

Figure 1. Geologic and tectonic map of southern Baja California (Lopez Ramos, 1976).

Late Miocene volcanic eruptions, apparently located along the margin on the eastern side of the peninsula (Rusnack and Fisher, 1964), are responsible for covering Miocene marine formations with the above deposits (Allison, 1964). Although principally visible in the study area along the eastern side of the peninsula, north of 23.75°N Lat., the Comondu volcanics also appear on the peninsula's southeastern tip and on islands in the Gulf of California.

The crystalline rocks on the southern end of the peninsula cover a large portion of the land surface of the study area and are considered to have the same origin as outcrops of the Peninsular Range Batholith found north of 28°N Lat. (Allison, 1964). Normark and Curray's (1968) study of seismic reflection profiles, over the continental margin adjacent to Baja California's southern tip, show the granitic batholith underlying Tertiary volcanics and marine sediments. Ultramafic crystalline rocks and serpentines along the western border of Magdalena and Almejas Bays are Mesozoic in age and are distinctly different from the rocks of the Peninsular Range Batholith (Allison, 1964).

Two major sedimentary formations overlie the volcanics and crystalline rocks. The Pliocene Salada Formation, consisting of sands, sandstones, calcareous clays and fossiliferous conglomerates, occurs on Baja California's southeast tip and at isolated areas along the peninsula's western side. These deposits are both marine and continental in origin. Pleistocene to Recent alluvium covers much of

the western coastal area of the peninsula and extends east to La Paz Bay across a narrow sedimentary province, which Bryne and Emery (1960) called the Isthmus of La Paz.

The vast majority of the study area's surface is covered by geologic features already discussed. However, various other sedimentary formations of Miocene and Eocene age occur at isolated sites along the length of the map. The Miocene San Raymundo Formation, visible primarily along the west coast of La Paz Bay, consists of shale and marine sandstones deposited in a coastal environment. Deposits of this formation are located at the southern tip of Baja California and in the vicinity of 24.4°N Lat., 111.2°W Lon. Near this latter position, Miocene rocks, identified as San Ignacio and Monterrey Formations, and the Eocene Tepetate Formation also contribute to the surface geology. The first contains sandstones, volcanic tuffs and fossiliferous conglomerates in coastal marine facies. The Monterrey Formation reveals both neritic and bathyal marine deposits of siliceous shale, diatomites, sandstones and mudstones. The Tepetate Formation consists of sandstones, shale, and traces of limestone deposited in coastal and neritic marine environments.

NEW DATA

Data Description and Location

During Project Baja-75, personnel of the OSU Geophysics Group and the Direccion General de Oceanografia collected gravity, magnetic, and bathymetric data along approximately east-west tracklines across the western continental margin of Baja California. During Project Baja-76, personnel involved in the joint effort made the same measurements in the Gulf of California, between Guaymas and Mazatlan, and seismic reflection and refraction measurements on the shelf west of the peninsula.

Figure 2 shows Baja-75 and Baja-76 tracklines within the study area, tracklines from other OSU cruises and submarine pendulum gravity stations from Worzel (1965). The R/V Yaquina, on separate cruises during the years 1971-72 and 1973-74, collected gravity, magnetic and bathymetric data along the four northwest trending tracklines that lie farthest offshore of Baja California. In January, 1976 the R/V Wecoma, while on its maiden voyage from Sturgeon Bay, Wisconsin, obtained additional gravity measurements on a trackline adjacent and approximately parallel to the four Yaquina lines. The shaded areas locate land gravity measurements compiled by the Defense Mapping Agency Aerospace Center (DMAAC).

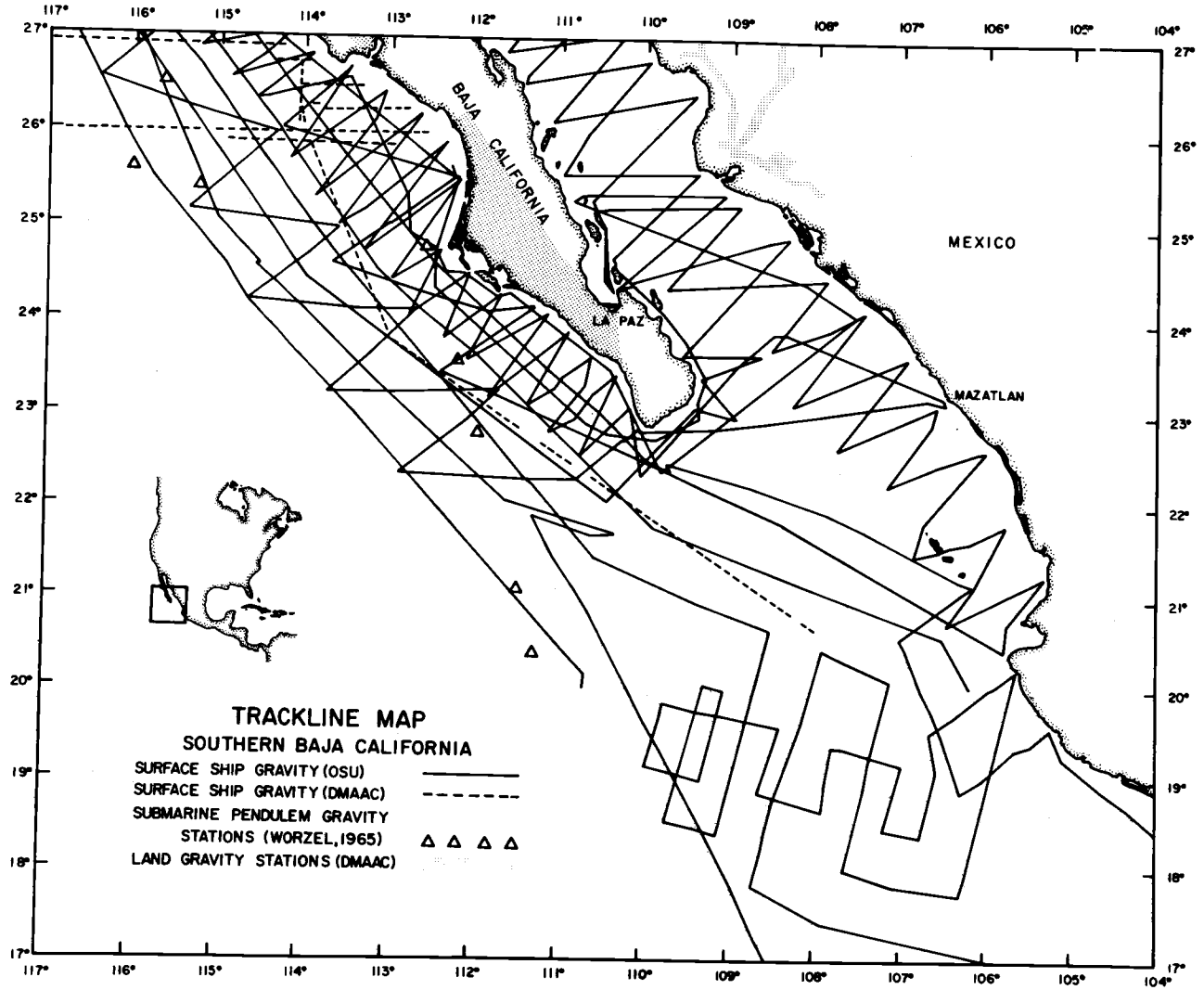

Figure 2. Location of gravity field measurements (OSU, DMAAC, Worzel, 1965). Surface ship tracklines also include magnetic and bathymetric measurements.

Data Acquisition and Reduction

Gravity

LaCoste and Romberg Surface Ship Gravity Meter S-42, mounted on a stable platform, provided the means for gravity data acquisition on all of the cruises. This meter recorded relative gravity measurements continuously on strip charts and magnetic tape. During the 1973-74 R/V Yaquina cruise (YALOC-73) and the Baja-75 cruise, these analog records were hand digitized at five minute intervals, except where rapid changes in the gravity field necessitated shorter intervals. On the other three cruises, digital gravity was recorded automatically every 30 seconds and later reduced to five minute intervals (G. Connard, OSU, personal communication). Depending upon ship speed, this sampling frequency yielded approximately one data point every 1.2 to 1.5 km.

LaCoste (1967) discussed the measurement of gravity at sea with a surface ship meter. The following is a summary of his discussion. In order to measure gravity with an accuracy of 1 milligal (1 milligal = 1×10^{-3} cm/sec^2) while on a continuously undulating sea surface, the gravity meter and its support systems must perform several tasks automatically. The meter has to maintain a level surface for the gravity sensor, which consists of a mass hinged about a horizontal axis and supported by a spring. In addition, the meter must

compensate for vertical and horizontal accelerations with magnitudes up to 100,000 times greater than the desired accuracy of 1 milligal (mgal). Other than by their characteristic frequencies, there is no way to distinguish between acceleration due to gravity and those due to the ship's vertical motion. Therefore, the relatively high frequency vertical accelerations, resulting from waves on the sea surface, are removed by applying a low pass filter to the electrical output of the meter. Horizontal accelerations produce a torque about the horizontal axis to which the mass of the gravity meter is hinged. The horizontal and vertical accelerations are thus coupled in the meter's equation of motion, and the result is called the cross-coupling effect. In meter S-42, an analog computer evaluates the magnitude of the torque and applies the necessary correction to the output.

Another factor that must be accounted for is the Eotvos Correction. This is the difference in gravity recorded by a meter at rest at a point on the earth's surface and gravity recorded when the meter is moving at a certain velocity over the same point. This correction has the following form for a meter moving on the sea surface.

$$E = (2V_{\phi}V_{e} + V^{2})/R_{\phi}$$

In this equation R_{ϕ} is the earth's radius at latitude ϕ. V_{ϕ} is the speed of rotation of the earth's surface, also at latitude ϕ, and V_{e} is the easterly component of the ship's total velocity, V (Heiskanen and

Vening Meinsesz, 1958). The first term is the vertical component of the Coriolis Force, and the second term is the centripital acceleration due to the ship's speed. A record of the changes in the Eotvos Correction, produced by course or speed changes, is superimposed on the gravity meter output.

Because the sea gravity meter records only relative differences in gravity, it was necessary to tie the sea measurements to land stations where absolute values of gravity have been established. The land ties were made by measuring the difference between gravity where the ship was docked and gravity at a nearby International Gravity Base Station. The survey crew used LaCoste and Romberg portable land meter G-126 for this purpose.

Table 1 lists land base stations that were used on Baja-75 and Baja-76. The 1975 cruise did not include the Guaymas station, but in the following year all were used. The DMAAC Reference Publication No. 25 (DMAAC, 1974) was the source for all the values except that at San Diego. The value at the San Diego station was obtained from Worzel (1965), where it was referenced as "f" Station. It was modified to reflect recent changes in the International Gravity Standardization Net (IGSN). The largest correction involved was the 14.4 mgal reduction of absolute gravity at the Washington, D.C. Commerce Building Pier Station. The new value for this station, to which all other stations in North America are referenced, is 980104.3 mgal.

Table 1. Gravity base stations used during Baja-75 and Baja-76.

Location	Gravity (mgal)	Source	Designation
San Diego	979517.7	Worzel (1965)	f
Ensenada	979446.64	International Gravity Bureau	12016C
Guaymas	979164.77	Universidad Nacional Autonoma de Mexico	23
La Paz	978907.94	"	28
Mazatlan	978838.84	"	34

Furthermore, in 1973 Oregon State University personnel compared gravity at Worzel's "f" Station with two other base stations, one at the San Diego Air Station and the other at Scripps Pier on Pt. Loma (M. Gemperle, OSU, personal communication). This comparison showed the value at the top of Table 1 to be in agreement with gravity at the other land stations.

Gravity data from YALOC-71 in the vicinity of Baja California were tied to San Diego and Acapulco gravity base stations. During YALOC-73 and the 1975-76 R/V Wecoma cruise (WELOC-75), gravity base stations provided absolute values at San Diego and at the Rodman Naval Station in the Panama Canal Zone. Woollard and Rose (1963) describe the base stations in Acapulco and the Canal Zone.

Besides establishing a base value for the relative gravity measurements, these land stations served to monitor the drift of

meter S-42. The total accumulated drift for the 47 day Baja-75 project was -4.7 mgal. The base station checks showed that the drift correction could be reasonably approximated by a straight line beginning with zero mgal at the start of the cruise and ending with the -4.7 mgal total drift observed upon return to San Diego. Two straight lines, one representing the drift between San Diego and Mazatlan and the other corresponding to the drift during the rest of the cruise, provided the drift correction for Baja-76. The total drift at the end of the 30 day Baja-76 project was -10.7 mgal.

Creating a navigation file was the first step in the reduction of data on shore. Satellite navigation was not available on Baja-75 or Baja-76, so the ship's crew relied on radar to establish the ship's position whenever it approached the coast. A dead reckoning navigation program, written by M. Gemperle (OSU), used course and speed information to locate the ship between consecutive radar fixes. The program also computed the ocean current velocity needed to make navigation, computed by dead reckoning, compatible with the radar fixes. The final step of the program recomputed the position of the ship as a function of time using the ocean current velocity as well as course and speed information. The computed ocean current and Eotvos Correction changes, produced by changes in ship speed and heading, were included in the output of the program. Comparison of this output with charted ocean current velocities and with Eotvos

Correction changes, observed on the output of the gravity meter, provided additional constraint on the computed navigation.

When this process was completed for the entire cruise, the navigation and geophysical data files were merged. During this step the merging program makes the Eotvos Correction and computes the free-air gravity anomaly. The International Gravity Formula provides a mathematical expression for gravity on a uniform rotating oblate spheroid that closely approximates the equilibrium sea level surface of the earth (International Association of Geodesy, 1971). The gravity from this formula provides a reference to which gravity on the real earth can be compared. The most recent version, adopted by the International Association of Geodesy in 1967, yields the following expression for gravity as a function of latitude, ϕ.

$$g = 987.03185(1 + 0.005278895 \sin^2 \phi + 0.000023462 \sin^4 \phi) \text{ gals}$$

For any measurement made at sea level, subtracting the reference spheroid gravity, called normal gravity, from the measured gravity generates the free-air anomaly. For land measurements, an additional elevation correction compensates for the fact that gravity decreases approximately as $1/r^2$ outward from the sea level surface.

Evaluating the difference in free-air anomaly values at trackline intersections provided an estimate of measurement uncertainties. A

calculation, based on differences found at trackline intersections in the study area, indicated a 3.6 mgal root-mean-square uncertainty in the measured values.

Magnetics

The International Geomagnetic Reference Field (IGRF), adopted in 1975 (International Association of Geomagnetism and Aeronomy, 1976), serves as a magnetic reference field to which real magnetic data can be compared. Subtracting the magnitude of the IGRF from the magnitude of the earth's field produces the total magnetic field anomaly. This anomaly, which is not the absolute value of the magnetic field due to an anomalous source, is defined as follows.

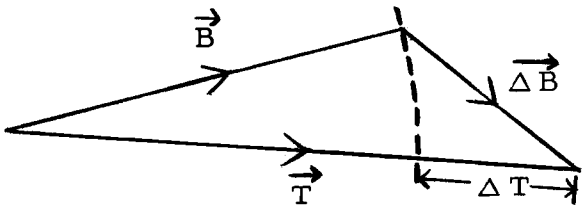

In the above diagram, $\vec{T}$ represents the earth's field, $\vec{B}$ is the reference magnetic field vector, and $\Delta\vec{B}$ is the field vector produced by an anomalous source. Because the magnetometer gives only the magnitude of the earth's field, the data do not contain enough information to determine $\Delta\vec{B}$. Instead, subtracting $|\vec{B}|$ from $|\vec{T}|$ generates the total magnetic field anomaly, ΔT (Blakely, USGS, personal

communication). A simple relationship between ΔT and $\overrightarrow{\Delta B}$ exists when $|\overrightarrow{\Delta B}| << |\vec{B}|$.

$$\Delta T \doteq \hat{B} \cdot \overrightarrow{\Delta B}$$

In the above expression $\hat{B}$ is the unit vector in the direction of the reference field vector. In the case of a magnetometer towed near sea level, $|\overrightarrow{\Delta B}|$ ranges between zero and a few hundred gammas, usually less than 500 gammas, while $|\vec{B}|$ is on the order of 50,000 gammas. This expression is therefore valid for the magnetic data used in this study.

Bathymetry

A 12 kHz acoustic signal, reflected from the ocean bottom and recorded on a single-channel graphic recorder, provided a continuous display of the ocean bottom topography on all the cruises. Members of the scientific crew hand digitized these records with a sampling interval of five minutes except where topography required more data points. After merging this information with the navigation file, a computer program, using data from Matthew's velocity tables (1939), converted the bathymetry from uncorrected fathoms to corrected meters.

Seismic Reflection and Refraction

A 40 in^3 airgun was the energy source for the seismic reflection profile across the western continental margin of Baja California. A hydrophone streamer, towed behind the ship, received the reflected signals, and a single-channel graphic recorder, set at a sweep rate of four seconds, displayed the information on paper. The airgun was also used for a reversed wide angle reflection and refraction line, located about 22 km northwest of the reflection profile. During measurement, hydrophone sonobuoys received reflected and refracted signals, while the ship, with the airgun in tow, moved away at a constant rate and heading. These signals were then radioed to the ship and displayed by a single-channel graphic recorder.

DATA INTERPRETATION

Free-Air Gravity Anomaly Map

Figure 3 shows a free-air anomaly map of the western margin of Baja California, based on the data discussed in the previous section. The map, contoured at 10 mgal intervals, has an overall estimated root-mean-square uncertainty of 3.6 mgal. The largest uncertainties occurred at trackline intersections farthest offshore (see Figure 2) where it was difficult to accurately establish the ship's position or motion.

The longest feature on the gravity map consists of the negative anomaly at the base of the continental slope and the positive anomaly at the outer edge of the shelf. This map and other preliminary free-air anomaly maps of central and northern Baja California (Calderon Riveroll, 1977; Coperude, 1977) show the feature to extend along the western margin south to about 22°50'N Lat. The maximum gradient across this feature occurs where the free-air anomaly ranges from -50 mgal to +40 mgal over a distance of approximately 15 km. The minimum values for the negative gravity anomaly are between -60 and -70 mgal at the base of the continental slope, while maximum values for the positive anomaly are between +40 and +50 mgal at the outer edge of the continental shelf.

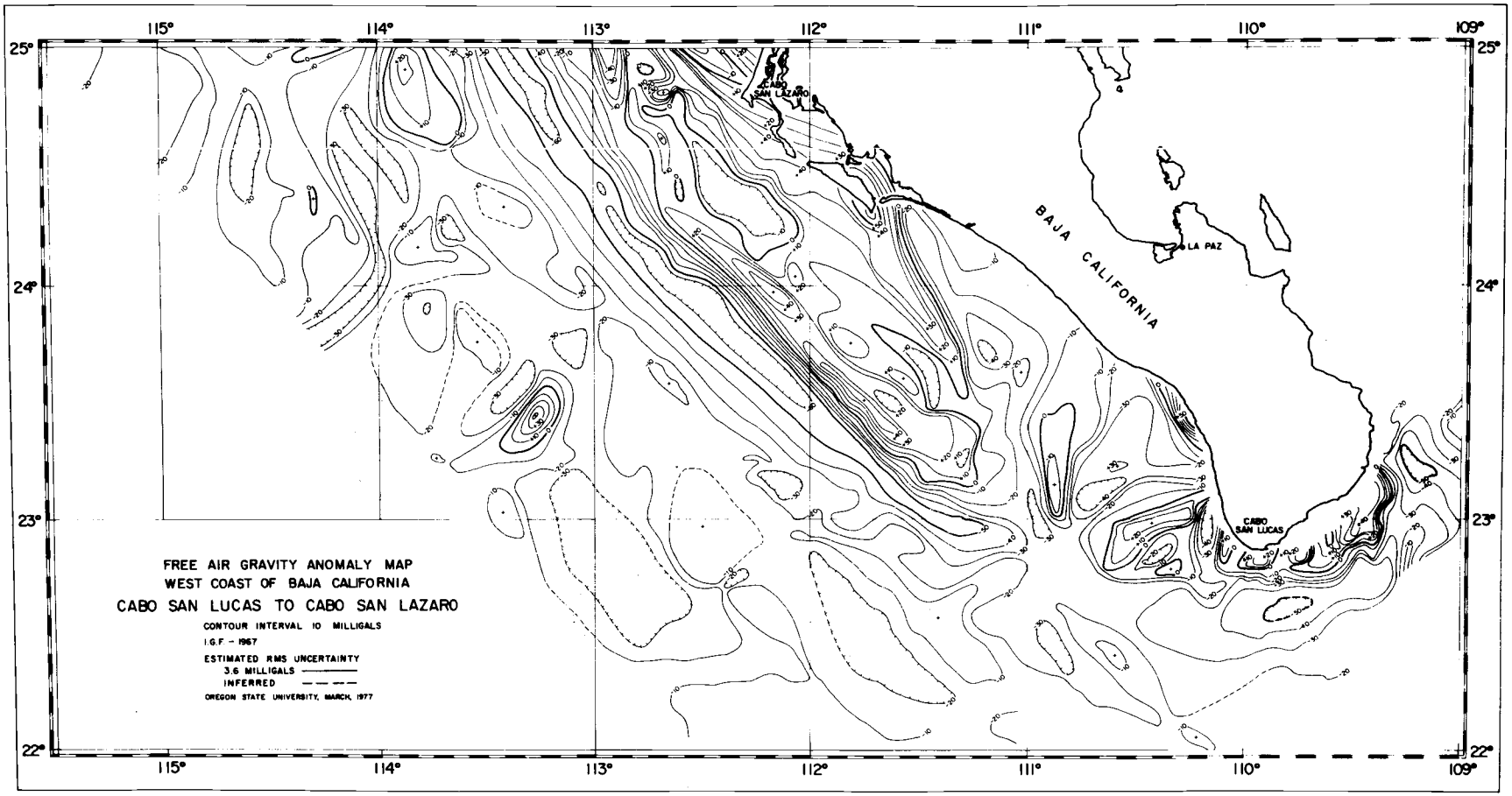

Figure 3. Free-air gravity anomaly map of the western continental margin of southern Baja California. Contour interval is 10 mgal.

Seaward of the shelf, the average free-air anomaly values are between -10 and -30 mgal. However, a positive anomaly, centered at 23.45°N Lat., 113.27°W Lon. reaches a maximum of +40 mgal. Existing bathymetric charts, prepared by Scripps Institution of Oceanography (U.S. Naval Oceanographic Office, 1971), show this to be coincident with a topographic feature rising from a depth of about 3.3 km to a peak at a depth of 2.2 km. The 20 mgal high at approximately 24.9°N Lat., 113.9°W Lon. also has a related topographic rise. The negative gravity anomaly that crosses 24°N Lat. at about 114°W Lon. marks the position of a group of small depressions in the ocean floor.

Over the outer edge of the shelf, two positive gravity anomalies that exceed +40 mgal are coincident with the outer shelf topographic high. Comparison with the reflection profile of Figure 7 shows that these 40 mgal anomalies locate an approximately 11 km wide block of sedimentary material uplifted about 200 meters relative to the shelf's surface immediately to the east. A depression in the shelf about 40 km long, 18 km wide and 200 meters deep, at its maximum depth, is associated with the negative anomaly centered at 24.3°N Lat., 112.3°W Lon. The free-air anomaly in this area decreases from a surrounding high of about 10 mgal to a low of -17 mgal. The magnitude of this negative anomaly suggests a local depression in the denser subsurface material, as the anomaly would not be so large if it was caused by just the absence of surface sedimentary material. The negative

anomaly, that crosses 25° N Lat. at 112° 55'W Lon., contains free-air anomaly values which decrease to less than -50 mgal just north of 25° N Lat. A structural depression of about 400 meters in the continental slope coincides with this anomaly.

Other than the free-air anomaly along the seaward edge of the continental shelf, the anomaly that extends through Magdalena and Almejas Bays is the most distinctive. Magdalena Bay is centered at approximately 24° 40'N Lat., 112°W Lon., and Almejas Bay lies southeast of it. From the north, a gravity anomaly gradient crosses these two bays and then strikes about south 30° east. Eventually it merges with the negative anomaly at the base of the continental slope. Free-air anomaly values across this feature range from a high of more than +30 mgal on the northwest side to a low of less than -40 mgal on the southeast side. The extreme gravity high associated with this anomaly is on the southern tip of Magdalena Island where values in excess of +60 mgal are recorded. This gravity anomaly, it is postulated, marks the seaward extension of the structure forming the islands that enclose Magdalena and Almejas Bays.

The 111°W meridian roughly separates regions of distinctly different free-air anomaly trend and wavelength. East of this line the outer shelf gravity high and the negative anomaly, marking the continental slope base, are not apparent like they are west of the line. Off the southern tip of Baja California, a negative gravity anomaly is

detected with a minimum of about -50 mgal. The -40 mgal contour of this negative anomaly approximately coincides with the 1000 and 1500 fathom bathymetric contours of Shepard (1964). Also distinctive are short wavelength anomalies, ranging between -40 and +40 mgal, that occur around the southern tip of Baja California. The negative anomalies around the southern tip coincide with the Tinaja Trough and the Cardonal, San Lucas and Santa Maria submarine canyons described by Shepard (1964).

Total Magnetic Field Anomaly Map

Figure 4 shows a map of the total magnetic field anomaly, contoured at 100 gamma intervals. In several areas over the deep ocean, trackline coverage is inadequate to define the anomalies, hence dashed lines are used to represent inferred values. However, on the shelf the data density is sufficient so that 100 gamma contours are made with confidence. The root-mean-square uncertainty estimate for this map, based on trackline crossing differences, is 21 gammas.

Several spacially small, large amplitude anomalies exist in the vicinity of the islands that enclose Magdalena and Almejas Bays. One of these anomalies at approximately $24^{\circ}50'$N Lat., $112^{\circ}35'$W Lon. exceeds 900 gammas. A magnetic anomaly marks the proposed seaward extension of the Magdalena and Almejas Bay islands, which the free-air anomaly map in Figure 3 also indicates. A distinctive magnetic

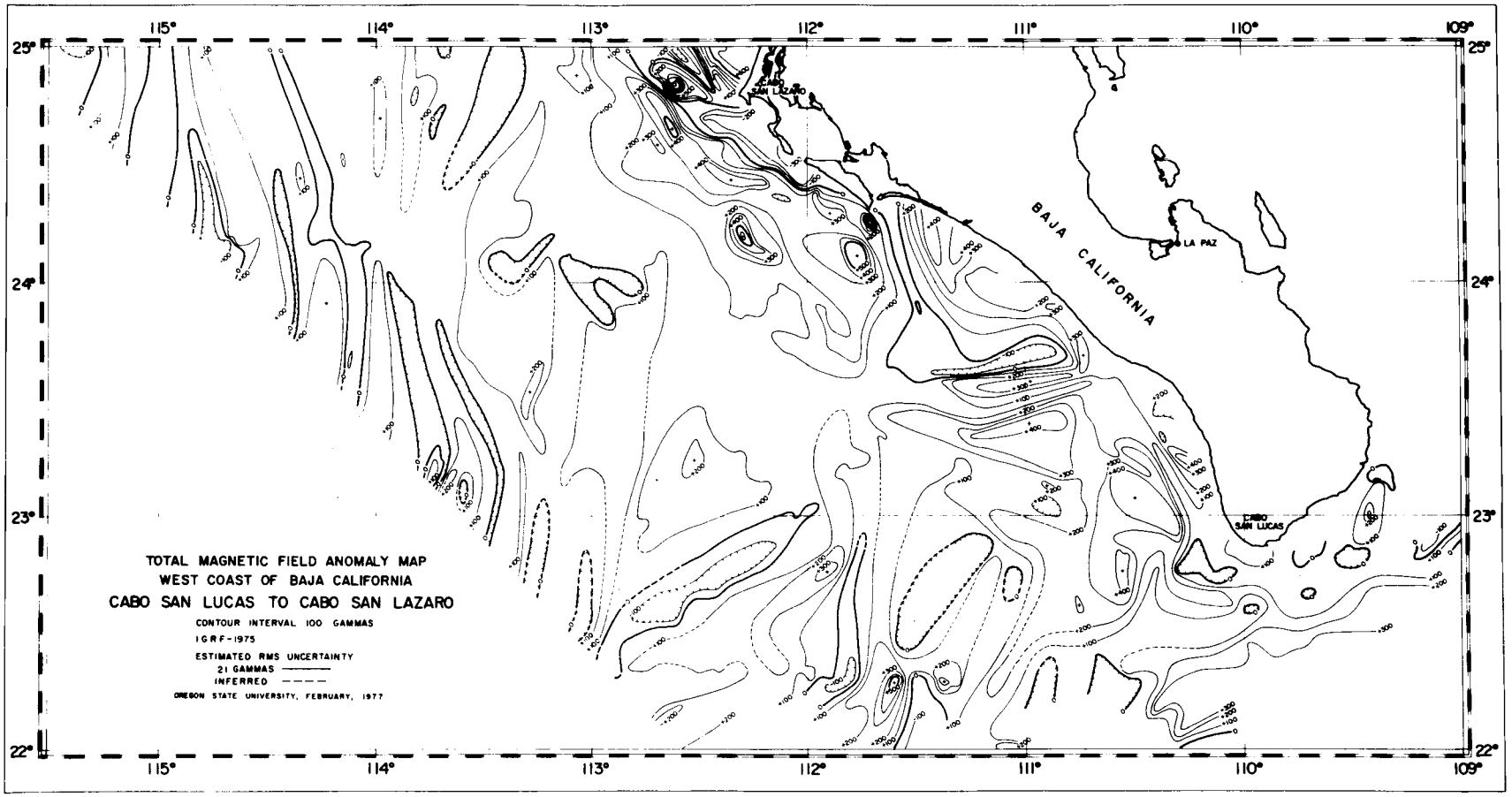

Figure 4. Total magnetic field anomaly map of the western continental margin of southern Baja California. Contour interval is 100 gammas.

anomaly, greater than 300 gammas, is centered approximately at 23.5° N Lat., 111°W Lon. Along a line extending south from this point, the anomaly first decreases to less than +100 gammas and then increases to over +400 gammas. North of the above coordinates a large negative gradient is apparent and the total magnetic field anomaly magnitude decreases to less than -100 gammas. The structure responsible for this magnetic effect does not have a noticeable influence on the gravity anomalies, nor is it visible on existing bathymetric maps. Consequently, the magnetic anomalies are the only significant indication of the presence of this major structural feature. The pattern of the magnetic anomalies suggests that their source is a fault or faults with vertical displacement and approximately east-west strike.

Continental Margin Bathymetry

Figure 5, a perspective view of the submarine topography extending out to the edge of the shelf off southern Baja California, shows clearly a line of vertical displacements in the shelf, something not easily detectable on a contour map of the area. The abrupt changes in the depth of the shelf, marked by the arrows in Figure 5, exceed 400 meters and are coincident with the free-air anomaly that trends southeast from Almejas Bay. The shelf surface seaward of the arrows correlates with a gravity anomaly greater than 30 mgal and is elevated compared to the shelf surface on the landward side where

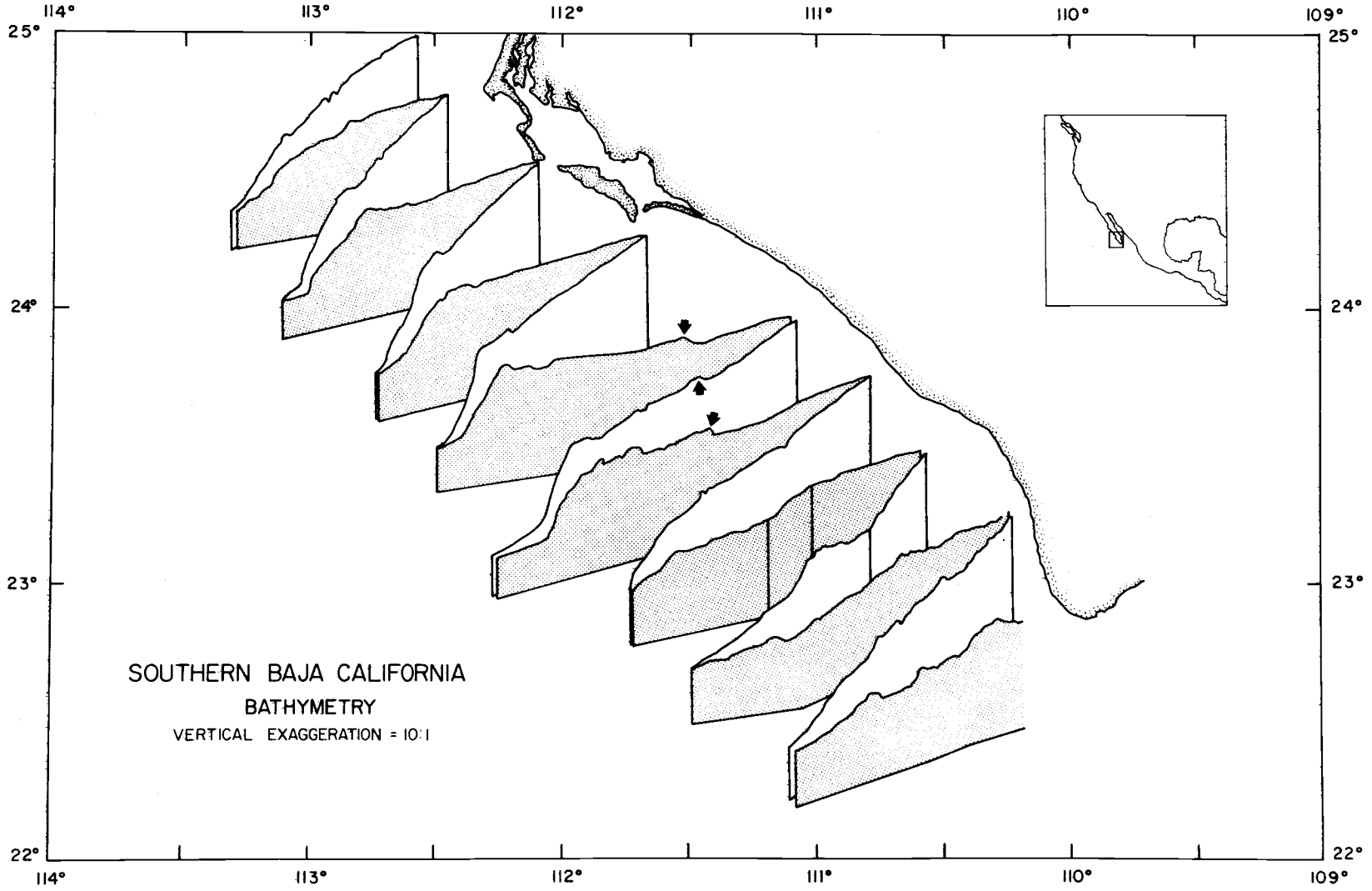

Figure 5. Perspective view of the continental margin bathymetry west of southern Baja California. Arrows indicate a line of vertical displacements in the depth of the shelf.

the free-air anomaly decreases to -40 mgal. The bathymetry displayed in Figure 5 suggests that the feature might be the result of relative vertical motion between two large fault blocks.

Figure 5 also shows a major change in the continental margin structure west of Baja California's southern tip. Unlike the bathymetric measurements along the northern and middle tracklines, which clearly show both continental shelf and continental slope, the bathymetric measurements from the southern-most lines do not show typical segments of a continental margin profile. This change in margin structure correlates with the previously discussed regional changes in the trend and wavelength of the free-air anomalies.

Seismic Reflection Profile

Figure 6 shows the location and orientation of seismic reflection profile BB', obtained during Baja-76, and model crustal section AA'. Also shown are the locations of the seismic refraction stations (McConnel and McTaggart-Cowen, 1963; Phillips, 1964; Shore et al., 1970) that were used as constraints in constructing cross section AA'. Line BB' lies approximately 53 km northwest of line AA', and both profiles are approximately normal to the northwest trend of Baja California. The Baja-76 sonobuoy refraction profile, 3-76, is about 22 km northwest of line BB'.

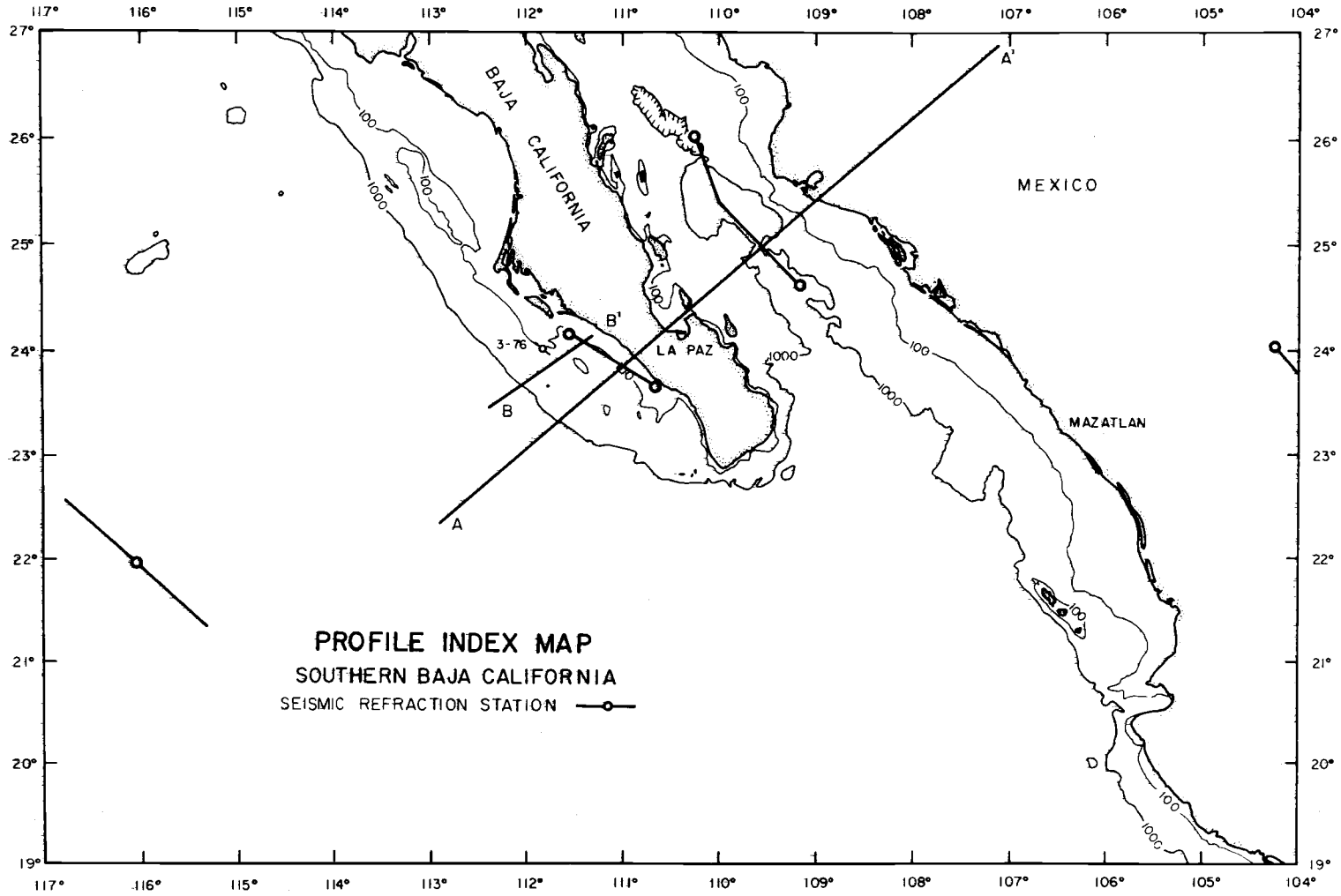

Figure 6. Profile index map. Lines AA' and BB' show the location and orientation of a crustal cross section and a seismic reflection profile, respectively. Seismic refraction stations are used to constrain cross section AA' (Shor et al., 1970; Phillips, 1964; McConnell and McTaggart-Cowen, 1963). Station 3-76 is a Baja-76 sonobuoy refraction station

Figure 7 is a line drawing of seismic reflection profile BB'. The vertical axis, which is proportional to signal travel-time, is marked in depth intervals of 1 km, assuming 1.5 km/sec for the water velocity. The horizontal axis is marked in 10 km increments beginning at the west end, and the discussion below refers to these distances. At the west end of the profile, the water is approximately 3.1 km deep, and assuming an average sediment velocity of 2.0 km/sec, the thickness of sediment above the acoustic basement is about 800 meters. East of 20 km and west of the continental slope base at 42 km, the acoustic basement and deep sediment layers dip toward the coast, while the surface sediment layers remain relatively horizontal. Between the continental slope base and the distance of about 52 km, the margin slopes upward toward the east at an angle of about 2.8°. East of 52 km the margin slopes upward at a maximum angle of 15.1° until reaching a depth of about 205 meters at the outer edge of the continental shelf.

The total continental shelf width along this profile is about 90 km. At 77 km, more than 200 meters of relative vertical displacement, probably by normal faulting, topographically separate the shelf's outer 11 km from the central shelf. Between 82 km and 100 km, the sediment cover is broken by normal faulting and the near emergence of older deformed sediments. Farther east, between 100 km and 123 km, smooth, relatively undisturbed sediment layers slope

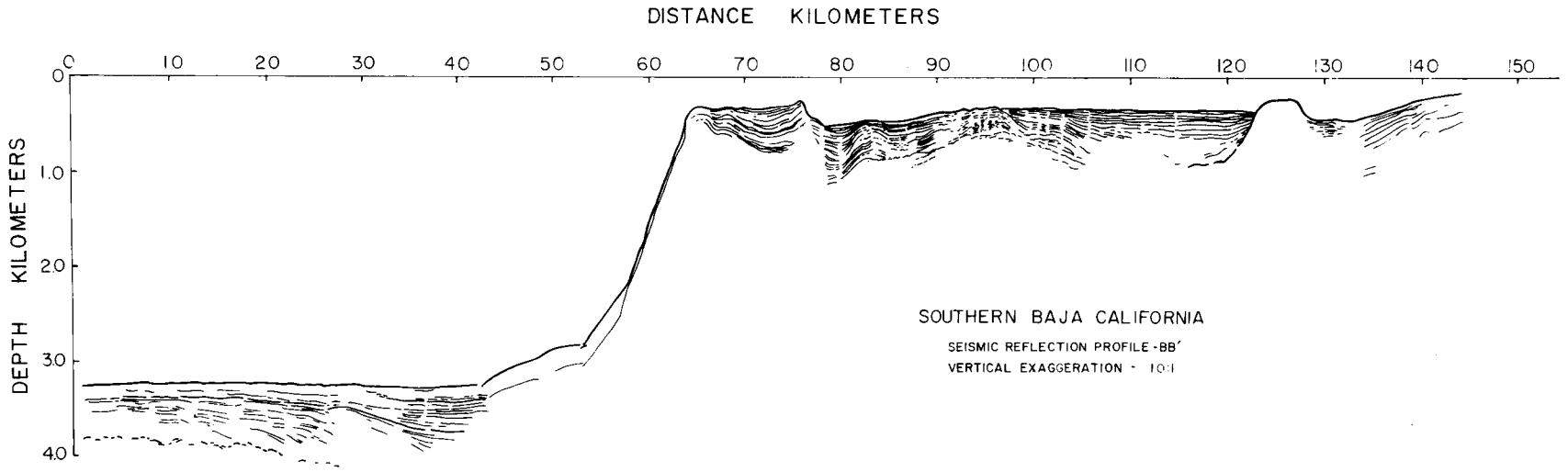

Figure 7. Seismic reflection profile BB'. The vertical scale in kilometers assumes 1.5 km/sec for the velocity of sound in water.

downward toward the east at an angle of about 0.2^{o}. At a profile distance of about 123 km, a 4 km wide rock structure is apparent. Its top surface is elevated approximately 200 meters above the shelf sediments immediately to the east. This structure lies beneath the elongate free-air anomaly, that trends southeast from Almejas Bay, and is the northwestward continuation of the vertical bathymetric displacements indicated by arrows in Figure 5. These gravimetric and bathymetric features are proposed to be indications of a submerged southeast extension of the structure that forms the Magdalena and Almejas Bay islands. The rock structure indicated by reflection measurements is interpreted to be the seaward extension of the island forming structure. Due to the reverberation of the acoustic signal, it is not possible to determine whether the upper part of the structure is sedimentary or exposed crystalline rock.

The surface of the sediment seaward of the 4 km wide structure lies about 70 meters above that on the landward side. Farther south along the trend of the structure, this vertical difference exceeds 400 meters. Wherever the ship tracklines cross this structure, the bathymetric profile shows the sequence as described below. Seaward of the coast, the shelf first deepens and then remains horizontal for several kilometers until the above structure is encountered. Up to as much as 25 km beyond the seaward side of the structure, the sediment cover is undisturbed and lies on the order of a few hundred meters

above the sediment cover on the landward side. The difference in sediment elevation could be the result of gravity faulting along a fault between the structure and the sediment on its landward side.

Reversed Sonobuoy Refraction Profile

Figure 8a and 8b shows the results of interpreting the Baja-76 reversed sonobuoy refraction study in terms of plane dipping layers of constant velocity. The shipboard recorder originally displayed the reflected and refracted signals on a graph that has both axes proportional to time. The abscissa is the time expired since the start of the profile and corresponds to the distance of the airgun source from the sonobuoy receiver. The ordinate is the time elapsed between the airgun blast and the arrival of the signal at the sonobuoy. The method of Le Pichon et al. (1968) is used to compute the velocity of the direct water wave from the first reflection hyperbola and the straight line that marks the direct wave arrival. This velocity and the direct wave line provide the necessary information to convert any particular signal's abscissa time to the distance between the airgun and the sonobuoy. Once this is done the refraction data can be graphed as signal travel-time versus horizontal distance traveled, as shown in Figure 8a. The solid circles are signal arrivals observed on the original record, and the straight lines represent the apparent seismic velocities of critically refracted waves which travel along different crustal layer boundaries.

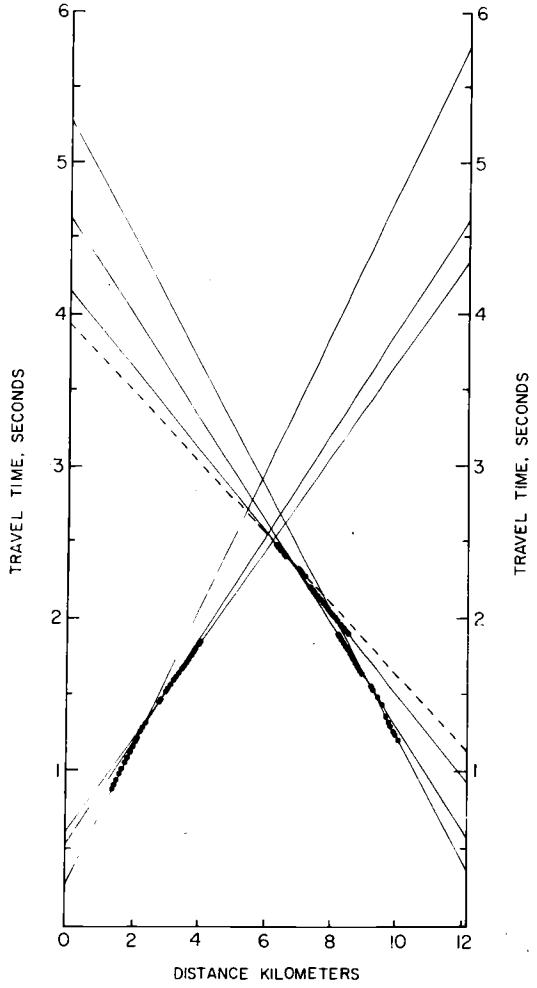

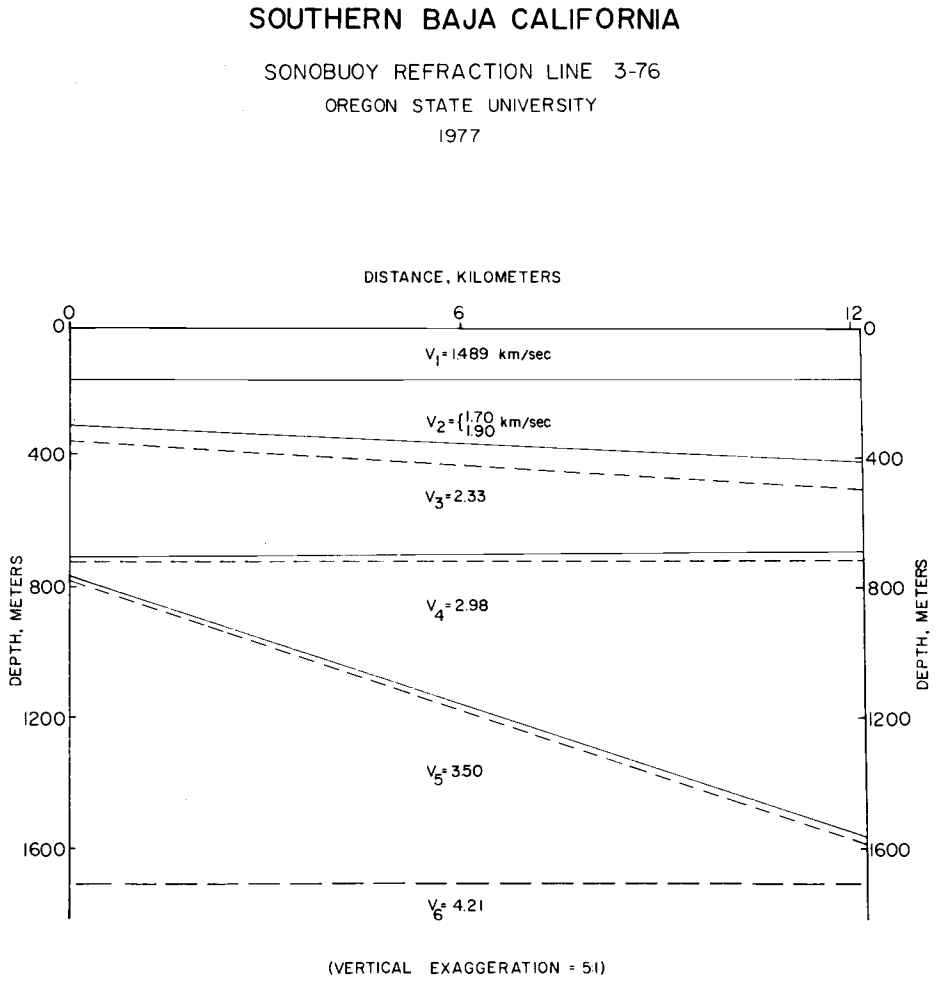

Figure 8a. Travel-time plot for the Baja-76 reversed sonobuoy refraction profile 3-76. Total length of the profile is 12.15 km.

Figure 8b. Layer depths and velocities indicated by refraction profile 3-76. Solution assumes plane dipping layers with constant velocity.

Except for providing the seismic velocity of the direct water wave via the method of Le Pichon et al. (1968), the wide angle reflection hyperbolas of the original record fail to give any useful information. The shallow water, in the area of sonobuoy profile 3-76, produces large amplitude multiples with short delay times, which interfere with the signals from subsurface acoustic reflectors. As a result, only the refraction arrivals are analyzed.

Because only a negligible amount of energy is refracted through the uppermost sediment layer, the problem of signal multiples leaves the velocity and thickness of this layer undetermined. Normally an analysis of the reflection hyperbolas would produce these values. To complete the refraction analysis, the velocity of this layer is assumed. Bathymetric data constrains the depth of the layer, and the intercept times of the paired straight lines, that mark the first detectable critical refraction, provide the final constraint needed to determine its thickness.

Given the assumed sediment velocity, the water velocity from Matthew's Tables (1939) and the water depth, the method of Adachi (1954) routinely determines the velocity, depth, and dip of each layer indicated by the graph in Figure 8a. This method requires that each crustal layer boundary produce a straight line on the travel-time vs. distance graph in both the forward and reverse directions. The physical model, upon which this method is based, further requires

identical forward and reverse end-to-end travel-times for a wave critically refracted between two crustal layers.

The dashed line in Figure 8a does not meet the first of the two conditions. This particular refraction arrival is detected in only one direction, so it is not included in the computation that uses the method of Adachi. Also, the solid lines in Figure 8a, that represent the forward apparent velocities, do not have the same travel-time axis intercepts as the corresponding lines in the reverse direction. Thus, the second condition is not rigorously satisfied. Adjusting the slopes of the lines in Figure 8a, so that corresponding reverse and forward lines have the same end-to-end travel-time, results in a five percent decrease in V_3 from the value computed below. The above changes for V_4 and V_5 from the values shown in Figure 8b are less than one percent, while changes in layer depths are approximately five to six percent.

A computer program, written by S. Johnson (OSU), computed via the method of Adachi the depths, dips and velocities of all but the bottom layer of the cross section shown in Figure 8b. The solid lines denote the solution if a 1.7 km/sec velocity is assumed for the upper sediment layer, and the short dashes represent the layer boundaries if the sediment velocity is 1.9 km/sec. A 1.8 km/sec sediment layer velocity, calculated from a refraction profile over the western continental shelf of Baja California at about 28.8°N Lat., 115°W Lon.

(Calderon Riveroll, 1977), suggests that the above range of velocities is reasonable. In Figure 8b the computed seismic velocities are listed in their respective layers. At the bottom of the cross section, long dashes mark the layer boundary responsible for the dashed line in Figure 8a. A computer program, also written by S. Johnson (OSU), computed the depth and velocity of the bottom layer based on the assumptions that the layer's upper boundary is horizontal and the upper sediment velocity is 1.7 km/sec. The same computation, but with 1.9 km/sec for the sediment velocity, does not produce significantly different results from the one presented by the long dashes. Tables 2a and 2b show the results of calculations for the two assumed sediment velocities. The computed velocities are very similar to those of another Baja-76 reversed refraction profile, located on the continental shelf at about latitude 25.6°N Lat. Though they are not as deep, all but the bottom layer of Figure 8b show no significant difference in their velocities from those of the corresponding layers, computed by the other study (Coperude, 1977).

Including the assumed upper sediment layer, the above analysis indicates at least five separate crustal layers compose the continental margin. However, a single layer with a positive velocity gradient might better represent the two layers with constant velocity immediately beneath the assumed layer. Data from the original record do not clearly distinguish between a discrete or continuous velocity

Table 2a. Plane dipping layer solution from program WAREFRA (see Appendix). Solution assumes an upper sediment velocity of 1.7 km/sec.

V2 = 1.70 KM/SEC
N = 6 SPREAD = 12.1

N	APPARENT VELOCITY	DIP	LAYER THICKNESS AT ORIGIN
1	1.489	0	.160
2	1.700	0	.254
3	2.337	.532	.273
4	2.932	-0.092	.378
5	3.497	3.757	.141
6	4.333	0	

N	DEPTH A	THICK A	VELOCITY	THICK B	DEPTH B
1	.160	.160	1.489	.160	.160
2	.415	.254	1.700	.141	.302
3	.688	.273	2.337	.405	.707
4	1.565	.378	2.932	.060	.767
5	1.707	.141	3.497	.939	1.707
6			4.21		

Table 2b. Plane dipping layer solution from program WAREFRA (see Appendix). Solution assumes an upper sediment velocity of 1.9 km/sec.

V2 = 1.90 KM/SEC
N = 6 SPREAD = 12.1

N	APPARENT VELOCITY	DIP	LAYER THICKNESS AT ORIGIN
1	1.489	0	.160
2	1.900	0	.336
3	2.334	.704	.221
4	2.932	-0.026	.371
5	3.497	3.807	.135
6	4.333	0	

N	DEPTH A	THICK A	VELOCITY	THICK B	DEPTH B
1	.160	.160	1.489	.160	.160
2	.496	.336	1.900	.187	.347
3	.717	.221	2.334	.376	.723
4	1.588	.871	2.932	.056	.779
5	1.723	.135	3.497	.943	1.723
6			4.21		

gradient. The top of the 3.50 km/sec layer is much more definite, because it appears as a very distinct refraction arrival. The bottom layer boundary, assumed to have zero dip, is not as well constrained as the boundary immediately above it but is included in the cross section to indicate that a crustal layer, with a velocity of about 4.2 km/sec, occurs at a depth of approximately 1700 meters.

Southern Baja California Cross Section

Figure 9 displays the crustal and subcrustal cross section constructed along line AA' of Figure 6. This profile, oriented normal to the trend of Baja California, begins at the end of a trackline about 270 km southwest of the peninsula. It crosses Baja California just north of the city of La Paz, spans the Gulf of California, and extends about 300 km into mainland Mexico. The numbers indicate layer densities in gm/cm^3, and the black bars denote layer depths determined from seismic refraction profiles, whose locations are shown in Figure 6. The solid curve immediately above the cross section indicates the observed free-air anomaly along line AA', and the open circles are the free-air anomaly values computed by the method of Talwani et al. (1959). The upper-most curve and the one just below it denote the observed and theoretical total magnetic field anomaly profiles, respectively.

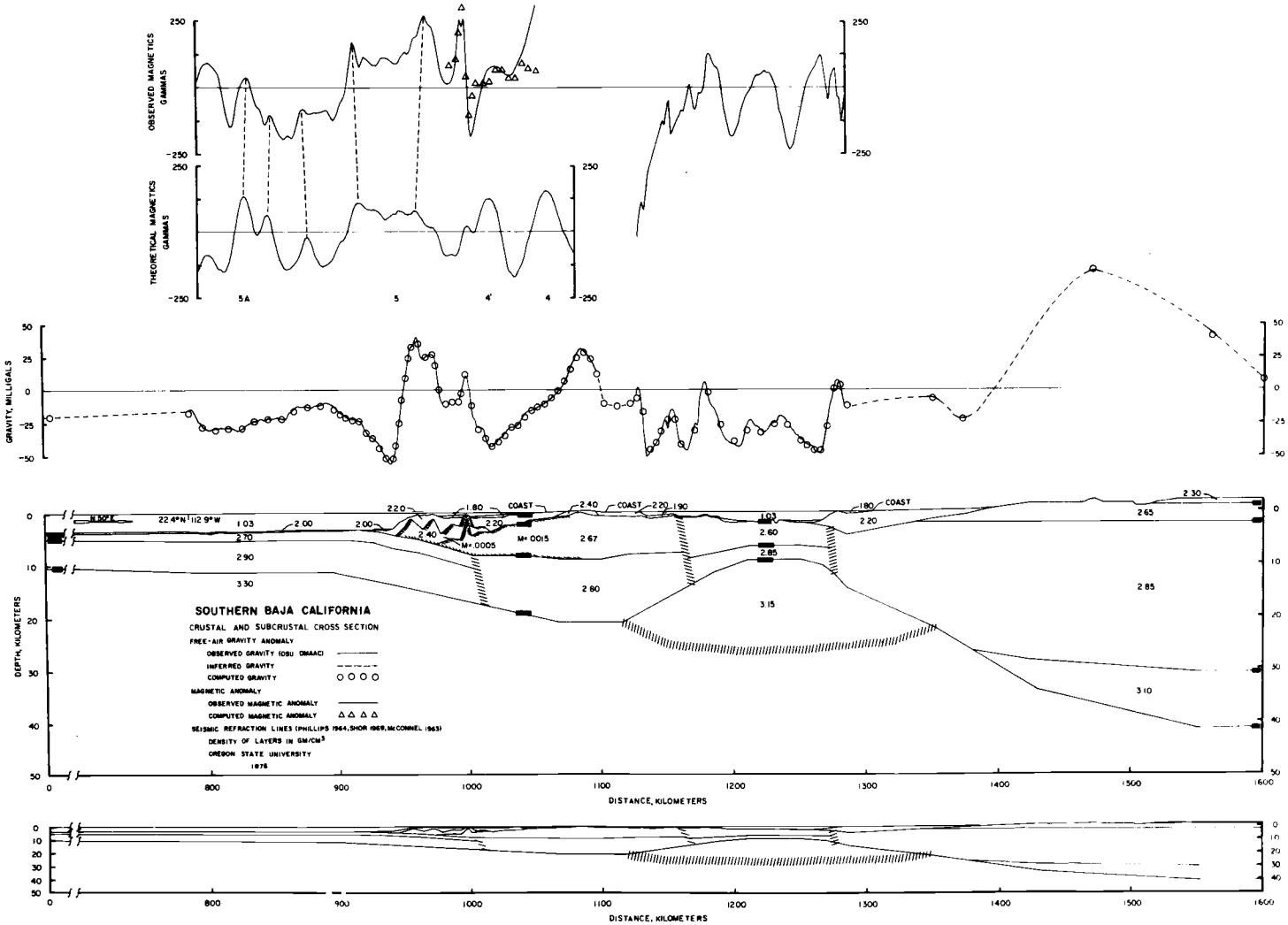

Figure 9. Southern Baja California crustal and subcrustal cross section. Profile is along line AA' of Figure 6. The upper and lower cross sections have vertical exaggerations of 4:1 and 1:1, respectively.

Between the left end of the profile and the negative gravity anomaly at the base of the continental slope, the free-air anomaly ranges between -30 and -10 mgal. The wide relative gravity high, centered approximately at the cross section distance marked 900 km, coincides with a gentle rise in the ocean bottom topography. The negative gravity anomaly at the base of the continental slope reaches the lowest free-air anomaly value for the cross section, -55 mgal. Landward of the continental slope base, the free-air anomaly increases until attaining a maximum of slightly more than +40 mgal over the outer edge of the continental shelf. The proposed seaward extension of the structure that forms the Magdalena and Almejas Bay islands is responsible for the gravity anomaly peak landward of the outer shelf gravity high. Farther toward the east, the free-air anomaly decreases to -45 mgal, then increases to a maximum of +30 mgal at the middle of Baja California. In the Gulf of California the free-air anomaly along profile AA' is almost entirely negative and averages approximately -25 mgal. Bathymetric highs in the gulf correlate with the gravity anomaly highs.

Comparison of the observed and theoretical total magnetic field anomaly profiles at the top of Figure 9 shows correlation from 12.7 m.y. at the west ends of the profiles, through anomaly 5, and up to 8.5 m.y. at the cross section distance marked 1000 km. At the 1000 km distance, a magnetic anomaly associated with structure

predominates. A computer program, developed by Lu and Keeling (1974), generated the theoretical curve from the magnetization of an infinite horizontal slab at a depth of 4 km. The paleomagnetic time scale of Blakely (1974) and a half spreading rate of about 4.0 cm/yr yields the magnetization of the slab. The 4.0 cm/yr spreading rate is in the range of rates listed by Atwater (1970) and Chase et al. (1970). When projected on the latter's map of magnetic anomaly lineations, the position of anomaly 5A in Figure 9 lies within 10 km of the anomaly 5A line shown on the map. The correlation of the theoretical and observed profiles suggests that the observed magnetic anomalies are Pacific Plate remanent anomalies generated by sea-floor spreading. As such, they indicate oceanic crustal age decreasing from 12.7 m.y. to 8.5 m.y. between the cross section distances labeled as 800 km and 1000 km.

The remanent magnetic anomalies of cross section AA' extend approximately 50 km landward of the edge of the shelf. At the distance marked 1000 km, a large amplitude, short wavelength magnetic anomaly, which coincides with the proposed extension of the Magdalena and Almejas Bay islands, interrupts the remanent magnetic anomaly sequence and dominates the observed magnetic profile. A computer program, written by R. Blakely (USGS), uses the method of Talwani and Heirtzler (1964) to compute the total magnetic field anomaly resulting from the magnetization of two dimensional polygonal bodies.

The triangles show values, computed in the above manner by assuming induced magnetization of the two subsurface crustal blocks outlined by small, closely spaced hachures. The parameter M, listed within the crustal blocks, denotes magnetization in EMU/cm^3, estimated from susceptibility measurements of rocks with similar physical characteristics (Lindsley et al., 1966).

The first step in the construction of this model is the adoption of a mass column from which the model's free-air anomaly can be computed. The mass column is established by a standard oceanic section above which the free-air anomaly is zero. Determinations of the gravitational attraction of oceanic sections, constrained by various seismic refraction stations, have shown that no unique standard section applies everywhere in the world (Barday, 1974). Most sections are computed to a depth of 50 km, below which the mantle is assumed not to have any lateral variations in density. The differences in standard sections imply lateral imhomogeneities in the mantle exist below the lower boundary of the sections. Therefore, the selection of a standard section is somewhat arbitrary, but Barday (1974) considered factors such as crustal age and geographic location. The average standard section of Barday (1974) is computed from an area reasonably close to the present study area. Furthermore, the crustal age, at this profile's western-most seismic refraction station, is 18 m.y. This age lies in the 17 m.y. to 42 m.y. range of crustal ages

used by Barday (1974) to arrive at a standard section. For these reasons, the gravitational attraction from his standard section, 6442.0 mgal, is adopted as the value corresponding to zero free-air gravity for the southern Baja California crustal and subcrustal cross section.

Layer depth and velocity determinations from seismic refraction measurements, bathymetric data and land topography from World Aeronautical Charts (U.S. Air Force, 1969) constrain the model. The seismic velocities are converted to densities with the use of the Ludwig, Nafe and Drake curve (1970, Fig. 11). Tables 3a and 3b list the seismic refraction data, beginning with the western-most refraction constraint of Figure 9 and proceeding in order toward the east. In these tables, T and V indicate layer thickness and layer velocity, respectively. The densities (D) are selected to be compatible with the empirical relationship between velocity and density of Ludwig et al. (1970) and to yield a gravitational attraction consistent with the observed free-air anomaly over the station. Gravity data are lacking at the first seismic station, but submarine pendulum measurements (Worzel, 1965) in the general area suggest the gravity anomaly is about -20 mgal. This is in agreement with a free-air anomaly map generated from satellite orbit observations (Gaposchkin and Lambeck, 1971). A gravity anomaly value of -20 mgal is therefore assigned to the first refraction station. To obtain

Tables 3a and 3b. Seismic refraction data and assigned densities.[1]

Water			Sediment			Transition			Oceanic			Mantle		
T	V	D	T	V	D	T	V	D	T	V	D		V	D
Table 3a														
	3.83	1.495	1.03	0.32	2.15	2.00	0.97	5.38	2.70	5.31	6.78	2.90		8.24	3.30

Water		1			2			3			4			5			Mantle	
T	D	T	V	D	T	V	D	T	V	D	T	V	D	T	V	D	V	D
Table 3b																		
0.15	1.03	0.50	1.70	1.80	1.60	2.90	2.20	6.10	5.00	2.67	11.20	6.10	2.80				7.90	3.30
2.00	1.03	0.42	2.00	1.80				3.20	4.78	2.60	2.52	6.16	2.85				7.74	3.15
					0.80	3.00	2.25	3.40	5.00	2.65	28.50	6.00	2.85	10.70	7.60	3.10	8.40	3.30

[1] Data in Table 3a from Shore et al. (1970). Data in Table 3b from the following sources: first two rows from Phillips (1964; last row from McConnell and McTaggart-Cowen (1963).

T = thickness in km; V = velocity in km/sec; D = density in gm/cm^3

this value the model assumes a transition layer density of 2.70 gm/cm^3, an oceanic layer density of 2.90 gm/cm^3 and an upper mantle density of 3.30 gm/cm^3. Barday's section (1974) uses 2.60, 2.90 and 3.32 gm/cm^3, respectively, for these layers.

The layer depth and velocity solution for the gulf station was one of two proposed by Phillips (1964). The one shown in Figure 9, with a two layer crust, is used as it is more representative of the majority of seismic refraction measurements made at sea than his single layer crust solution. Figure 6 shows that the mainland Mexico seismic refraction station is about 400 km from line AA'. Projecting the station's results northwest along the trend of the refraction profile provides a constraint for the east end of the cross section. Because of the large distance involved in the projection, the station's relevance to the cross section is somewhat questionable. However, both the mainland Mexico refraction station and the intersection of its profile trend with line AA' lie in the same geologic province. This refraction station provides the best available information for constructing a realistic mainland Mexico crust consistent with land gravity measurements. Farther west, where the seismic refraction profiles actually cross line AA', the cross section is better constrained.

Starting at the west end of the section, where the upper mantle is at a depth of 10.4 km, the Moho deepens gradually toward the continental shelf. Approximately 40 km west of the continental slope

base, the dip of the Moho steepens to 3.1° until the Moho reaches a maximum depth of 21 km directly beneath Baja California. Immediately east of the peninsula, the Moho dips toward the west, at an angle of approximately 7.7°, and under the Gulf of California it attains a minimum depth of 9.2 km. Below the east side of the gulf, the boundary between crust and mantle deepens in coincidence with the mainland Mexico continental slope. Beneath the Mexican mainland, the Moho is at its maximum depth for cross section AA', 43.4 km.

The density estimate for the upper mantle material beneath the Gulf of California is 3.15 gm/cm^3. Fitting the negative free-air anomaly values over the gulf requires the above value, which is lower than that of the surrounding mantle material (3.30 gm/cm^3). The existence of this lower than average mantle density is consistent with the continuation of the East Pacific Rise into the Gulf of California (Talwani et al., 1965; Dehlinger et al., 1970). Hachures along the lower boundary of the low density zone indicate the uncertainty of its dimensions. Without better seismic refraction control an accurate determination of the extent and complexity of this zone is not possible.

Similar hachures represent the transition from oceanic crust beneath the Gulf of California to the continental crust of Baja California and mainland Mexico. The fracture zone map of Moore

(1973), which indicates areas composed of new crust, provides constraint for the east and west extent of the gulf crust.

The 2.40 gm/cm^3 continental margin material west of Baja California and the material covering the peninsula's surface are included in this model without the confirmation of the seismic refraction data in Tables 3a and 3b. There are factors, however, that necessitate their inclusion. Geologic maps (e.g., King, 1969; Lopez Ramos, 1976) show that much of southern Baja California is covered by Tertiary volcanics consisting primarily of Miocene andesitic, pyroclastic, and related epiclastic rocks. These rocks are similar in composition and age to the volcanics of the western Cascade Range in Oregon, where a reduction density for the Bouguer Correction is found to be about 2.40 gm/cm^3 (Blank, 1968). Based on this information, the density estimate for the volcanics covering Baja California is 2.40 gm/cm^3. The second block of material, also assigned a density of 2.40 gm/cm^3, is situated in the peninsula's western continental margin beneath 2.20 gm/cm^3 material. The inclusion of a crustal block, with density greater than 2.20 gm/cm^3, is required by the free-air anomaly. The bathymetric relief alone does not account for the magnitude of the relatively high frequency gravity anomalies over the outer shelf. Modeling these requires a structure of denser subsurface material within the continental margin. Additional evidence for the existence of this crustal block comes from the Baja-76

sonobuoy refraction line, located about 75 km northwest of line AA' (see Figure 6). The 3.50 km/sec and 4.21 km/sec layers, listed in Tables 2a and 2b indicate an average density of about 2.40 gm/cm^3, based on the Ludwig et al. (1970) empirical relationship between velocity and density. These two layers lie beneath a layer with a velocity of approximately 3.00 km/sec (Table 2a and 2b), which corresponds to a density of 2.20 gm/cm^3. The above sequence of continental margin densities is the same one used in crustal cross section AA'.

The continental margin structure, at the distance marked 1000 km in Figure 9, represents the seaward extension of the structure that forms the Magdalena and Almejas Bay islands. According to cross section AA', the material visible at the top of the structure is the 2.40 gm/cm^3 sedimentary material and not the 2.67 gm/cm^3 crystalline rock. As was noted in the discussion of Figure 7, the seismic reflection record does not reveal whether the exposed material is crystalline or sedimentary. Thus, a possible alternative to the structure, shown in Figure 9, is one with the block of 2.67 gm/cm^3 material protruding through the surface of the shelf.

Also at approximately 1000 km from the west end of the model, hachures mark the transition from oceanic crust of the Pacific Plate to 2.80 gm/cm^3 crust beneath Baja California. With respect to the tectonic evolution of the area, this extension of oceanic crust under the

continental crust of the peninsula is a significant feature of the cross section. The excellent correlation of theoretical and observed magnetic anomaly profiles indicates the presence of oceanic crust under the continental shelf. The correlation between these two magnetic profiles ceases with a magnetic anomaly that is produced by the structure discussed in the last paragraph. Because there is no physical evidence for extending the oceanic crust beyond this point, the model assumes a transition from oceanic to continental crust, and this is marked by the hachures. However, it is possible that the oceanic crust does not end at this point but continues all the way under Baja California into the Gulf of California. This possibility and the tectonic implication of Pacific Plate oceanic crust under western Baja California are discussed below.

DISCUSSION

Near Surface Continental Margin Structure

Comparison of the free-air anomaly map and the seismic reflection profile shows that the negative gravity anomaly at the base of the continental slope is above an area where the acoustic basement deepens and the sediment layer thickens. What is observed on the reflection profile is the sediment filled remnant of the trench that once was active just off the coast of western North America. At the outer edge of the shelf, an approximately 11 km wide block of sedimentary material, uplifted more than 200 meters, correlates with a positive gravity anomaly that exceeds +40 mgal. Farther landward on the reflection profile, a 4 km wide structure coincides with a prominent free-air anomaly that trends southeast from Magdalena and Almejas Bays. This structure, portrayed by the perspective bathymetric display of Figure 5, shows vertical displacement striking southeast from the above bays. The elevated sediments on the seaward side of the structure are coincident with free-air anomaly values between +30 and +40 mgal. The magnitude of the free-air anomaly rapidly decreases in the landward direction across the strike of the vertical displacements (Figure 5) and reaches a minimum of -40 mgal above the topographically depressed area on the structure's landward

side. Based on the above observations, the 4 km wide structure, revealed by the seismic reflection profile, is proposed to be the seaward extension of the structure that forms the islands enclosing Magdalena and Almejas Bays. This submerged feature intersects the cross section of Figure 9 at approximately the distance indicated on the section as 1000 km.

The total magnetic field anomaly map shows a +400 gamma magnetic anomaly centered at about 23.4°N Lat., 111°W Lon. Along a line extending north of this point, the total magnetic field anomaly magnitude rapidly decreases to less than +100 gammas, then increases to over +300 gammas, and finally decreases to less than -100 gammas. Vertical displacement along a fault or faults, with approximately east-west strike, may cause this magnetic anomaly pattern. However, neither gravity nor bathymetry give any positive indication of a fault, and until another survey is made over the area, the existence of the fault remains speculative. A seismic reflection profile across the magnetic anomaly may determine the structure of the anomaly's source, or perhaps the trend of the anomaly could be projected to a fault visible on land.

Geologic Cross Section

The model crustal cross section in Figure 9 represents Baja California's western continental margin by three blocks of different

densities. It indicates values of 1.80 gm/cm^3 for an approximately 300 to 400 meter thick upper sediment layer and 2.20 gm/cm^3 for a second layer, both of which are constrained by Phillips' (1964) refraction profile. Seaward of Phillips' refraction profile, the model also includes a deeper block of crustal material with a density of 2.40 gm/cm^3. The magnitude of relatively short wavelength gravity anomalies over the shelf requires this additional layer of continental margin material, and the Baja-76 refraction profile, 3-76, located about 75 km northwest of the cross section, also indicates the layer's presence. The refraction line actually suggests four or five separate layers in the margin, two of which have velocities greater than the 2.9 km/sec layer of Phillips (1964). Because refraction profile 3-76 does not coincide directly with cross section AA', these relatively thin sedimentary layers are omitted in the model. Instead, an average density of 2.40 gm/cm^3 represents the two layers with velocities greater than that of the 2.20 gm/cm^3 layer (2.9-3.0 km/sec). In Figure 10 a geologic interpretation of the cross section, based on the generalized geology shown in The Tectonic Map of North America (King, 1969), associates these two densities with metasediments and Tertiary to Quaternary sediments, respectively.

The shaded area in Figure 10 indicates Pliocene to Holocene oceanic crust beneath the Gulf of California. This, the youngest crust in the section, is in the vicinity of spreading centers of the East

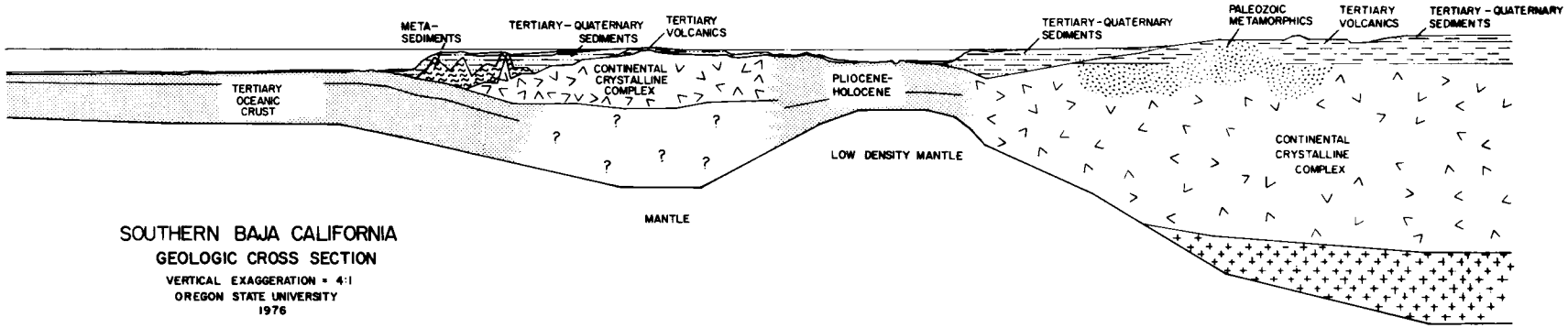

Figure 10. Geologic interpretation of cross section AA' based on The Tectonic Map of North America (King, 1969).

Pacific Rise. Low density mantle material, immediately beneath the oceanic crust, is consistent with the presence of the ocean ridge system (Talwani et al., 1965; Dehlinger et al., 1970). As indicated by the model cross section of Figure 9, the estimated density of this material is 3.15 gm/cm^3, while that of the surrounding mantle is 3.30 gm/cm^3. The maximum thickness of the low density zone is about 17 km, but other combinations of density and thickness are possible. Although the zone's boundaries and density are not entirely certain, they illustrate the fact that negative free-air anomaly values in the Gulf of California require a decrease in mantle density over a large region.

Figure 10 further shows that Baja California is overlain by Tertiary volcanics of the Comondu Formation. The material immediately underneath is collectively termed the Continental Crystalline Complex. This classification includes rocks of the Peninsular Range Batholith visible on the southern tip and in central and northern Baja California. The lower crustal material is not identified for reasons that are explained below. The maximum computed thickness of Baja California for this cross section is approximately 21 km.

Seaward of Baja California, magnetic surveys (Atwater, 1970; Chase et al., 1970) establish the shaded oceanic crust of Figure 10 to be late Tertiary, ranging in age from about 18 m.y. at the west end to 8.5 m.y. directly beneath the last identified magnetic anomaly of

Figure 9. The boundary between the oceanic crust and the continental crust west of Baja is very much dependent upon the identification of the magnetic anomalies over the shelf. Significantly, the remanent magnetic anomalies, associated with sea-floor spreading, do not cease at the edge of the continental shelf but extend at least 50 km landward. Their magnetized source, the oceanic crust, must therefore do the same. The geologic section in Figure 10 shows this crust dipping beneath the continental shelf and extending landward as far as the magnetic anomalies indicate. Any lateral boundary between it and the continental crust, if one exists at all, is uncertain. Oceanic crust may, for example, exist all the way under Baja California, making a continuous layer from the Pacific Ocean into the Gulf of California.

Tectonic History

The eastward continuation of oceanic crust beneath the western continental shelf of Baja California has important implications concerning the manner of the late Oligocene to late Miocene collision of the East Pacific Rise with the trench that existed west of North America prior to the collision. The magnetic anomalies of Figure 9, with their age continuously decreasing toward land, indicate that their magnetized source was formed west of the East Pacific Rise, i.e., the source constitutes part of the Pacific Plate oceanic crust. Because the relative motion between the North American and Pacific

Plates in western North America is right-lateral strike-slip, this observation of Pacific Plate oceanic crust beneath Baja California requires explanation.

Atwater (1970) states that the formation of the boundary between the Pacific and North American Plates followed the path of a migrating ridge-trench-transform triple junction. She contends the collision of the East Pacific Rise and the North American trench resulted in a transform fault along the axis of the former trench. This type of boundary implies a cessation of ridge spreading, for had the spreading continued, the boundary could not have been the transform fault as Atwater described. She further suggests that after this boundary cooled and strengthened, the relative motion of the two plates began to occur at weaker sites in the crust, of which some present-day examples are the San Andreas fault and the transform faults of the Gulf of California. The implication is that the ridge was inactive for a time, having ceased its spreading upon collision with the trench and not beginning again until its re-emergence in the Gulf of California. To account for the Pacific Plate oceanic crust beneath the western continental margin of Baja California, Atwater's hypothesis must assume that the peninsula overrode the Pacific Plate sometime after the East Pacific Rise reached North America.

Another explanation, which the present study favors, proposes that the spreading centers of the East Pacific Rise remained active

after reaching the trench and continued to form Pacific Plate oceanic crust on their west side, as they migrated under the North American Plate. Unlike the previous hypothesis, this one does not require a period of oblique Pacific Plate subduction beneath Baja California to account for the feature in question. Instead, the oceanic crust beneath the western continental margin of the peninsula is considered to have been placed there by the descending but still active spreading centers of the East Pacific Rise. Thus, with the above process, it is possible to have Pacific Plate oceanic crust beneath Baja California with no relative plate motions other than the presently observed right-lateral motion. Observations of crustal deformation of Baja California follow quite reasonably from consideration of the stresses generated as the peninsula, while still attached to the North American Plate, moved laterally over Pacific Plate oceanic crust. This hypothesis further suggests that the separation of Baja California from the North American Plate began as the oceanic crust beneath the peninsula strengthened and became "welded" to continental crust.

CONCLUSIONS

Gravity, magnetic, seismic and bathymetric data, collected during the cruises, Baja-75 and Baja-76, reveal the structure of the crust and upper mantle in the vicinity of southern Baja California. On the continental shelf west of Baja California, the above data indicate a structure that begins north of 25°N latitude and extends south through Magdalena and Almejas Bays. At the southern boundary of Almejas Bay this structure strikes approximately south 30° east across the shelf for a distance of about 105 km. It is concluded that this constitutes a submerged extension of the structure forming the Magdelena and Almejas Bay islands. Magnetic data reveal the presence of a major shelf structure, centered at approximately 23.5°N Lat., 111°W Long. Vertical displacement along a fault or faults with approximately east-west strike is assumed responsible for the magnetic anomaly at the above coordinates. It is suggested that future seismic reflection profiles across the magnetic anomaly or an attempt at correlating the trend of the anomaly with faults on Baja California may substantiate this hypothesis.

Seaward of Baja California's western continental shelf, the Moho is between 10 and 11 km deep and lies beneath late Tertiary oceanic crust. Below the negative gravity anomaly at the base of the continental slope, the acoustic basement and sediment layers

immediately above the acoustic basement dip toward land. At this point the Moho also deepens toward the continent, eventually reaching a maximum depth of approximately 21 km under Baja California. Negative gravity anomalies over the Gulf of California require Pliocene to Holocene crust to overlie low density mantle material whose upper boundary has depth as shallow as 9.2 km. Situated in a region where the presence of the East Pacific Rise is established (e.g. Menard, 1960; Von Herzen, 1963; Thatcher and Brune, 1970), this zone of low mantle density is consistent with similar zones indicated by crustal and subcrustal models of mid-ocean ridges (Talwani et al., 1965; Dehlinger et al., 1970).

Analysis of the recently collected data also has important implications for the tectonic history of southern Baja California. Marine magnetic anomalies, resulting from sea-floor spreading, extend at least 50 km landward of the edge of the peninsula's western continental shelf. This observation requires oceanic crust to be present at least that far under the continental margin. Furthermore, identification of the anomalies reveals that their ages decrease continuously in the landward direction and thus establishes the oceanic crust to be part of the Pacific Plate. This study proposes that the oceanic crust was placed under Baja California as the spreading centers of the East Pacific Rise migrated under the peninsula. This process is more continuous than the one described by Atwater (1970),

which, to account for the above feature, requires a period of oblique subduction of the Pacific Plate beneath Baja California.

An interesting speculation is that the above late Tertiary crust might form a continuous layer under Baja California from the Pacific Ocean to the Gulf of California. Spreading rates, based on magnetic anomalies west of the peninsula, the estimated age difference between Pacific and gulf crusts, and the distance across the peninsula suggest this possibility. If this hypothesis is correct, it accounts for the East Pacific Rise spreading centers between the time of their collision with the trench west of Baja California and their appearance in the gulf. However, the hypothesis does not explain why Baja California broke from the North American Plate in the particular configuration that it did. This question of crustal separation may be related to the protogulf (Moore, 1973) or other tectonic features that could be interpreted as weaknesses in the crust.

BIBLIOGRAPHY

Adachi, R. 1954. On a proof of fundamental formula concerning refraction method of geophysical prospecting and some remarks. Kumamoto Journal of Science, Serial A, v. 2:18-23.

Allison, E.C. 1964. Geology of areas bordering Gulf of California. In: Marine Geology of Gulf of California. T.H. van Andel and George G. Shor (eds.), Tulsa, American Association of Petroleum Geologists. p. 3-29.

Atwater, T. 1970. Implications of plate tectonics for the Cenozoic tectonic evolution of western North America. Geological Society of America Bulletin 81:3515-3536.

Atwater, T. and P. Molnar. 1973. Relative motion of the Pacific and North American Plates deduced from sea-floor spreading in the Atlantic, Indian and South Pacific Oceans. In: Proc. Conf. Tectonic Problems San Andreas Fault System, Geological Science Series 13. R.L. Kovack and A. Nur (eds.). Stanford, California, Stanford University. p. 136-148.

Barday, R.J. 1974. Structure of the Panama Basin from marine gravity data. M.S. thesis. Oregon State University, Corvallis. 99 pp.

Byrne, J.V. and K.O. Emery. 1960. Sediments of the Gulf of California. Geological Society of America Bulletin 71(7):983-1010.

Blakely, R.J. 1974. Geomagnetic reversals and crustal spreading rates during the Miocene. Journal of Geophysical Research 79:2927-2985.

Blank, H.R., Jr. 1968. Aeromagnetic and gravity surveys of Crater Lake Region, Oregon. In: Andesite Conference Guidebook. Bulletin 62, Hollis M. Dole (ed.), Portland, State of Oregon Department of Geology and Mineral Industries, p. 42-52.

Calderon Riveroll, G. 1977. A marine geophysical study of Vizcaino Bay and the continental margin of western Baja California. M.S. thesis. Oregon State University, Corvallis. (in preparation)

Chase, C.G., H.W. Menard, R.L. Larson, G.F. Sharman and S.M. Smith. 1970. History of sea-floor spreading west of Baja California. Geological Society of America Bulletin 81:491-498.

Coperude, S. 1977. Geologic structure of the western continental margin of south central Baja California based on seismic and potential field measurements. M.S. thesis. Oregon State University, Corvallis. (in preparation)

Defense Mapping Agency Aerospace Center. 1974. World Relative Gravity Reference Network North America, Part 1. St. Louis, Department of Defense.

Dehlinger, P., R.W. Couch, D.A. McManus, and M. Gemperle. 1970. Northeast Pacific structure. In: The Sea. v. 4, Part II. A. Maxwell (ed.), New York, John Wiley and Sons, p. 133-189.

Gaposchkin, E.M. and K. Lambeck. 1971. Earth's gravity field to the sixteenth degree and station coordinates from satellite and terrestrial data. Journal of Geophysical Research 76(20):4855-4883.

Hamilton, W. 1961. Origin of the Gulf of California. Geological Society of America Bulletin 64:443-458.

Harrison, J.C. and S.P. Mathur. 1964. Gravity anomalies in Gulf of California. In: Marine Geology of Gulf of California. T.H. van Andel and George G. Shor (eds.), Tulsa, American Association of Petroleum Geologists. p. 76-89.

Heiskanen, W.A. and F.A. Vening Meinsesz. 1958. The Earth and Its Gravity Field. New York, McGraw Hill, 470 pp.

Hilde, T.W.C. 1964. Magnetic profiles across Gulf of California. In: Marine Geology of Gulf of California. T.H. van Andel and George G. Shor (eds.), Tulsa, American Association of Petroleum Geologists. p. 122-125.

International Association of Geodesy. 1971. Geodetic Reference System 1967. Bulletin of Geodesy Special Publication, No. 3:116 pp.

International Association of Geomagnetism and Aeronomy. 1976. International Geomagnetic Reference Field 1975. EOS, Transactions of the American Geophysical Union 57(3):120-121.

King, P.B. 1969. Tectonic Map of North America. Washington, D.C., U.S. Geological Survey.

LaCoste, L.J.B. 1967. Measurement of gravity at sea and in the air. Geophysics 5(4):477-526.

Larson, P.A., J.D. Mudie, and R.L. Larson. 1972. Magnetic anomalies and fracture zone trends in the Gulf of California. Geological Society of America Bulletin 83:3361-3368.

Larson, R.L., H.W. Menard, and S.M. Smith. 1968. Gulf of California: A result of ocean-floor spreading and transform faulting. Science 161:781-784.

Lee, W.H.K. 1970. On the global variations of terrestrial heat-flow. Physics of the Earth and Planetary Interiors 2(51):332-341.

Le Pichon, X. 1968. Sea-floor spreading and continental drift. Journal of Geophysical Research 73(12)3661-3697.

Le Pichon, X., J. Ewing, and R. Houtz. 1968. Deep sea sediment velocity determination made while reflection profiling. Journal of Geophysical Research 73(3):2597-2614.

Lindsley, D.H., G.E. Andreasen, and J.R. Balsley. 1966. Magnetic properties of rocks and minerals. In: Handbook of Physical Constants. S.P. Clark, Jr. (ed.), New York, Geological Society of America. p. 543-552.

Lopez Ramos, E. 1976. Carta Geologica de la Republica Mexicana. Mexico City, Comite de la Carte Geologica de Mexico.

Lu, R.S. and K.M. Keeling. 1974. A simplified program for the rapid calculation of theoretical marine magnetic anomalies. Science Reports of the National Taiwan University, no. 4:105-114.

Ludwig, W.J., K.E. Nafe, and C.L. Drake. 1970. Seismic refraction. In: The Sea. v. 4, Part I. A. Maxwell (ed.), New York, John Wiley and Sons, Inc. p. 53-84.

Matthews, D.J. 1939. Tables of the velocity of sound in pure water and sea water for use in echo-sounding and sound ranging. Publ. H.D. 282. Admiralty Hydrogr. Dep., London. 52 pp.

McConnell, R.K., Jr. and G.H. McTaggart-Cowen. 1963. Crustal seismic refraction profiles: a compilation. Toronto, University of Toronto Institute of Earth Sciences.

McKenzie, D.P. and W.J. Morgan. 1969. Evolution of triple junctions. Nature 224: 125-133.

McKenzie, D.P. and R.L. Parker. 1967. The North Pacific: An example of tectonics on a sphere. Nature 216:1276-1280.

Menard, H.W. 1960. The East Pacific Rise. Science 132(3441): 1737-1746.

Menard, H.W. 1966. Fracture zones and offsets of the East Pacific Rise. Journal of Geophysical Research 71(2):682-685.

Minster, J.B., T.H. Jordan, P. Molnar, and E. Haines. 1972. Numerical modeling and instantaneous plate tectonics (abs.), 9th Annual Symposium on Geophysical Theory and Computers, Banff.

Molnar, P. 1973. Fault plane solutions of earthquakes and directions of motion in the Gulf of California and on the Rivera Fracture Zone. Geological Society of America Bulletin 84:1651-1658.

Moore, D.G. 1973. Plate-edge deformation and crustal growth, Gulf of California structural province. Geological Society of America Bulletin 84:1883-1906.

Moore, D.G. and E.L. Buffington. 1968. Transform faulting and growth of the Gulf of California since the late Pliocene. Science 161:1238-1241.

Morgan, W.J. 1968. Rises, trenches, great faults, and crustal blocks. Journal of Geophysical Research 73:1959-1982.

Normark, W.R. and J.R. Curray. 1968. Geology and structure of the tip of Baja California. Geological Society of America Bulletin 79:1589-1600.

Phillips, R.P. 1964. Seismic refraction studies in the Gulf of California. In: Marine Geology of Gulf of California. T.H. van Andel and George G. Shor (eds.), Tulsa, American Association of Petroleum Geologists. p. 90-121.

Reichle, M., G. Sharman, and J. Brude. 1976. Sonobuoy and teleseismic study of Gulf of California transform fault earthquake sequence. Geological Society of America Bulletin 66:1623-1641.

Rusnak, G.A. and R.L. Fisher. 1964. Structural history and evolution of the Gulf of California. In: Marine Geology of Gulf of California. T.H. van Andel and George G. Shor (eds.), Tulsa, American Association of Petroleum Geologists. p. 144-156.

Rusnak, G.A., R.L. Fisher, and F.P. Shepard. 1964. Bathymetry and faults of Gulf of California. In: Marine Geology of Gulf of California. T.H. van Andel and George G. Shor (eds.), Tulsa, American Association of Petroleum Geologists. p. 59-75.

Shepard, Francis P. 1964. Chart I: Submarine canyons - Cape San Lucas area, Mexico. Marine Geology of Gulf of California. T.H. van Andel and George G. Shor (eds.), Tulsa, American Association of Petroleum Geologists.

Shor, G.G., Jr., H.W. Menard, and R.W. Raitt. 1970. Structure of the Pacific Basin. In: The Sea. v. 4, Part II. A. Maxwell (ed.), New York, John Wiley and Sons. p. 3-27.

Talwani, M., J.L. Worzel, and M. Landisman. 1959. Rapid gravity computations for two-dimensional bodies with application to the Mendocino submarine fracture zone. Journal of Geophysical Research 64(1):49-59.

Talwani, M. and J.R. Heirtzler. 1964. Computation of magnetic anomalies caused by two-dimensional structures of arbitrary shapes. In: Computers in the Mineral Industries. Stanford University Publications. Vol. IX, no. 1:464-480.

Talwani, M., X. Le Pichon, and M. Ewing. 1965. Crustal structure of midocean ridges. II: Computed from gravity and seismic refraction data. Journal of Geophysical Research 70:341-352.

Thatcher, W. and J.N. Brune. 1971. Seismic study of an oceanic ridge earthquake swarm in the Gulf of California. Royal Astronomical Society Geophysical Journal 22:473-489.

United States Air Force Aeronautical Chart and Information Center. 1969. World Aeronautical Chart. Index nos. 520, 521, 591.

United States Naval Oceanographic Office. 1971. Bathymetry Atlas of the Northeastern Pacific Ocean. N.O. Publication No. 1205N.

Vine, F.J. 1966. Spreading of the ocean floor: new evidence. Science 154:1405-1415.

Von Herzen, R.P. 1963. Geothermal heat flow in the Gulfs of California and Aden. Science 140:1207-1208.

Wilson, J.T. 1965. A new class of faults and their bearing on continental drift. Nature 207:343-347.

Woollard, G.P. and J.C. Rose. 1963. International gravity measurements. Menasha, Wisconsin, George Banta Co.

Worzel, J.L. 1965. Pendulum gravity measurements at sea 1936-1959. New York, John Wiley and Sons, Inc. 421 pp.

APPENDIX

APPENDIX

Computer listings of the following programs are contained in this Appendix. These programs are used in constructing crustal and subcrustal cross section AA' and in analyzing sonobuoy refraction profile 3-76. The authors' names are listed in parentheses.

GRAV2DLD: (Gemperle, M., OSU) Computes at various field points, the vertical gravitational component of two-dimensional polygonal bodies, based on the method of Talwani et al. (1959). Inputs are the field points, where gravity is desired, the density of the two-dimensional bodies and their cross sectional boundaries.

MULTLAY: (Johnson, S.H., OSU) Using the method of Adachi (1954), this program accepts apparent velocities and intercept times from the travel-time vs distance graph of a reversed refraction profile and computes a cross section of plane dipping layers, each with a constant velocity.

THEOMAG: (Lu, R. and K. Keeling, OSU) Employs the paleomagnetic time scale of Blakely (1974) to establish the magnetization of a slab, infinite in one dimension and of specified thickness, width and depth. This magnetized source is then used to produce a plot of the total magnetic field anomaly along a line parallel to the proposed direction of spreading. Inputs are the ages of the right and left edges of the slab, spreading rate, latitude of the spreading center that produced the slab, angle between the desired profile (spreading direction) and geographic north, depths to top and bottom of the slab, the magnitude of the remanent magnetization, and inclination and declination of the earth's magnetic field at the center of the profile.

TWOMAG: (Blakely, R.J., USGS) Uses the method of Talwani and Heirtzler (1964) to compute, at various field points, the total magnetic field anomaly produced by two-dimensional polygonal bodies. Inputs are the field points, where the total magnetic field anomaly is desired, the strike and cross sectional boundaries of the two-dimensional bodies, the magnitude, inclination and declination of magnetization, and the inclination and declination of the earth's magnetic field in the vicinity of the field points.

WAREFRA: (Johnson, S.H., OSU) The full purpose of this program is outlined in the computer listing. For the specific case to which it is applied in this study, the program accepts the cross section computed by MULTLAY and computes one additional deeper layer boundary based on the dashed line of Figure 8a. Inputs are the velocities, thicknesses and dips of the upper layers and the apparent belocity, intercept time and assumed dip of the desired layer boundary.

```
      PROGRAM GRAV2DLD
      COMMON PX(50),X(400),Z(400),TOT(50),TIT(50),PZ(50)
    1 FORMAT(A8,2I5)
    2 FORMAT(F5.0,I3,A8)
  900 FORMAT(1H ,A8,F10.2)
  301 FORMAT(2F8.0)
  200 FORMAT(' ',F8.1,F12.4,F12.2,F12.4)
  201 FORMAT('0',2(A8,3X),A8//)
      WRITE(61,202)
  202 FORMAT('02D GRAVITY MODEL  V2  -  2/12/75'/
     1   ' REQUIRES X, Z FOR EACH FIELD PT')
      PI=3.1415927
      PIT2=2.*PI
  100 READ(2,1)SAM,M,N
      IF(EOF(2))CALL EXIT
      DO 52 I=1,M
   52 READ(2,301)PX(I),PZ(I)
      CALL TIME(A111)
      CALL DATE(A112)
      WRITE(61,201)SAM,A111,A112
      DO90I=1,M
      TIT(I)=0.
   90 TOT(I)=.0
      DO106IN=1,N
      READ(2,2)RHO,J,SALT
      WRITE(61,900)SALT,RHO
      DO 300 I=1,J
  300 READ(2,301)X(I),Z(I)
      K=J+1
      X(K)=X(1)
      Z(K)=Z(1)
      SUM=.0
      DO101I=1,M
      DO5J=1,K
      Z(J)=Z(J)-PZ(I)
    5 X(J)=X(J)-PX(I)
      DO122J=1,K
      TH=ATAN2(Z(J),X(J))
      IF(Z(J).LT.0.)TH=TH+PIT2
      IF(J.NE.1)GOTO10
      TH1=TH
      GO TO 122
   10 TH2=TH
      L=J-1
      A=Z(J)-Z(L)
      B=X(J)-X(L)
      JJ=5
      IF(X(L).EQ.0.)JJ=1
      IF(X(J).EQ.0.)JJ=2
      IF(A.EQ.0.)JJ=3
      IF(B.EQ.0.)JJ=4
      IF(TH1.NE.TH2)GOTO19
      S=0.
      GOTO102
   19 IF(X(L).NE.0.)GOTO22
      IF(Z(L).NE.0.)GOTO22
      S=0.
      GOTO102
   22 IF(X(J).NE.0.)GOTO25
      IF(Z(J).NE.0.)GOTO25
      S=0.
```

```
      GOTO102
   25 GOTO(26,27,28,29,30),JJ
   26 V6=TH2-.5*PI
      IF(ABS(V6).GT.PI)V6=V6-SIGNF(PIT2,V6)
      S=(X(J)*X(J)*Z(L)/(A*A+X(J)*X(J)))*(V6+(A/X(J))*(ALOG(ABS(Z(L)))
     1-.5*ALOG(X(J)*X(J)+Z(J)*Z(J))))
      GOTO102
   27 V7=TH1-.5*PI
      IF(ABS(V7).GT.PI)V7=V7-SIGNF(PIT2,V7)
      S=(X(L)*X(L)*Z(J)/(A*A+X(L)*X(L)))*(V7-(A/X(L))*(ALOG(ABS(Z(J)))
     1-.5*ALOG(X(L)*X(L)+Z(L)*Z(L))))
      S=-S
      GOTO102
   28 V8=TH2-TH1
      IF(ABS(V8).GT.PI)V8=V8-SIGNF(PIT2,V8)
      S=Z(L)*V8
      GOTO102
   29 V=SQRT((Z(J)*Z(J)+X(J)*X(J))/(Z(L)*Z(L)+X(L)*X(L)))
      S=X(L)*ALOG((X(L)/X(J))*V)
      GOTO102
   30 T=X(J)-(Z(J)*B/A)
      U=B*A/(B*B+A*A)
      V=TH1-TH2
      IF(ABS(V).GT.PI)V=V-SIGNF(PIT2,V)
      W=(A/B)*.5*ALOG((Z(J)*Z(J)+X(J)*X(J))/(Z(L)*Z(L)+X(L)*X(L)))
      S=T*U*(V+W)
  102 SUM=SUM+S
      TH1=TH2
  122 CONTINUE
      DO103J=1,K
      Z(J)=Z(J)+PZ(I)
  103 X(J)=X(J)+PX(I)
      DUM=SUM*13.346
      TIT(I)=TIT(I)+DUM
      SUM=SUM*RHO*13.346
      TOT(I)=TOT(I)+SUM
  101 SUM=.0
  106 CONTINUE
      DO 1000 KT=2,M
 1000 TIT(KT)=TIT(KT)-TIT(1)
      TIT(1)=0.
      WRITE(61,200)(PX(I),PZ(I),TOT(I),TIT(I),I=1,M)
      GOTO100
      END
```

```
      PROGRAM MULTLAY
      DIMENSION W(20),V(20),VA(20),VB(20),ALPH(20),BETA(20), Q(20),
     1  A(20),B(20),TAI(20),TBI(20),HA(20),HB(20),DA(20),DB(20),P(20)
      DIMENSION TITLE(8)
C IF TBI INTERCEPT TIMES ARE NOT READ IN,INSERT A BLANK CARD WHERE THEY ARE
C  CALLED FOR IN THE DATA DECK.THEY WILL THEN BE COMPUTED BY FORMULA AFTER STEP
C  421.  IF THEY ARE READ IN, THEY WILL BE CHECKED FOR CONSISTENCY WITHIN 10 PC.
 402  PRINT 401
 401   FORMAT (1H1)
C  N=NUMBER OF LAYERS OR TRAVEL TIME SEGMENTS, X=END-TO-END SPREAD LENGTH.
      READ 405,N,X,(TITLE(I),I=1,6)
 405  FORMAT (I4,F8.0,6A8)
      IF (N) 640,640,407
 407  READ 410,(VA(I),I=1,N)
 410  FORMAT (9F8.0)
      READ 410, (VB(I),I = 1,N)
      TAI(1)= .0
      READ 410, (TAI(I),I=2,N)
      TBI(1)= .0
      READ 410, (TBI(I),I=2,N)
      PRINT 415,(TITLE(I),I=1,6),X
 415  FORMAT (2X,6A8,15HSPREAD LENGTH =    ,F8.0,//)
      PRINT 420
 420  FORMAT ( 2X,10HINPUT DATA //10X,5HLAYER,10X,8HAPPARENT , 10X,
     1 8HAPPARENT,10X,9HINTERCEPT, 9X,9HINTERCEPT / 23X,13HVELOCITIES, A
     2 5X,13HVELOCITIES, 8,7X,8HTIMES, A,10X,8HTIMES, B  //)
 421  DO 425 I = 2,N
      TBB = TAI(I) + X*(1./VA(I) - 1./VB(I))
      IF (TBI(I)) 422,422,423
 422  TBI(I) = TBB
      GO TO 425
 423  TAEND = TAI(I) + X/VA(I)
      TBEND = TBI(I) + X/VB(I)
      ERROR = ABSF(TAEND/TBEND - 1.)
      IF (ERROR - .10) 425,424,424
 424  PRINT 1424,I
1424 FORMAT (5X,     74HAPPARENT VELOCITY AND TIME INTERCEPT DATA ARE IN
     1CONSISTENT AT LAYER NUMBER    ,I2,/,7X,56HEND-TO-END TRAVEL TIMES D
     2IFFER BY MORE THAN 10 PERCENT.       ,//)
      GO TO 425
 425  CONTINUE
      PRINT1425, (I,VA(I),VB(I),TAI(I),TBI(I),I=1,N)
1425 FORMAT (I12,F22.2,F18.2,F17.4,F18.4)
      V(1) = (VA(1) + VB(1))*.5
      DO 570 M = 2,N
      K = 1
      ALPH(1) = ASINF(V(1)/VB(M))
      BETA(1) = ASINF(V(1)/VA(M))
      IF (M-2) 500,500,510
 500  A(1) = (ALPH(1) + BETA(1))*.5
      W(2) = (ALPH(1) - BETA(1))*.5
      V(2) = V(1)/SINF(A(1))
      GO TO 550
 510  A(1) = ALPH(1) - W(2)
      B(1) = BETA(1) + W(2)
 520  K = K+1
      VV = V(K)/V(K-1)
      P(K) = ASINF(VV*SINF(A(K-1)))
      Q(K) = ASINF(VV*SINF(B(K-1)))
      IF (K+1-M) 530,540,540
 530  A(K) = P(K) - W(K+1) + W(K)
```

```
      B(K) = Q(K) + W(K+1) - W(K)
      ALPH(K) = A(K) + W(K+1)
      BETA(K) = B(K) - W(K+1)
      GO TO 520
  540 A(K) = (P(K) + Q(K))*.5
      B(K) = A(K)
      W(K+1) = W(K) + (P(K) - Q(K))*.5
      ALPH(K) = A(K) + W(K+1)
      BETA(K) = B(K) - W(K+1)
      V(K+1) = V(K)/SINF(A(K))
  550 KK = K-1
      HHA=0.
      HHB = 0.
      DO 560 I = 1,KK
      HH = COSF(ALPH(I)) + COSF(BETA(I))
      HH = HH/V(I)
      HHA = HHA + HH*HA(I)
  560 HHB = HHB + HH*HB(I)
      R = V(K)/(COSF(ALPH(K)) + COSF(BETA(K)))
      HA(K) = R*(TAI(K+1) - HHA)
      HB(K) = R*(TBI(K+1) - HHB)
      DA(1) = HA(1)
      DB(1) = HB(1)
      DA(K) = DA(K-1) + HA(K)
      DB(K) = DB(K-1) + HB(K)
  570 CONTINUE
      DO 580 J = 2,N
  580 W(J) = W(J)*57.2958           +0.001
      PRINT 620
  620 FORMAT (/// 2X,18HCOMPUTED STRUCTURE  // 9X,5HLAYER, 6X,8HVELOCITY
     1 ,  6X,11HTHICKNESS A, 4X,11HTHICKNESS B, 8X,3HDIP,10X,7HDEPTH A,
     2   8X,7HDEPTH B  //)
      I = 1
      PRINT 625, I, V(I), HA(I), HB(I),DA(I), DB(I)
  625  FORMAT (I12,3F15.2,15X,2F15.2)
      NN = N-1
      PRINT 630,(I, V(I), HA(I), HB(I), W (I),DA(I),DB(I),I=2,NN)
  630 FORMAT (I12,6F15.2)
      PRINT 635,N, V(N), W (N)
  635 FORMAT (I12,F15.2,30X,F15.2)
      GO TO 402
  640 CONTINUE
      END
```

```
      PROGRAM THEOMAG
      COMMON /DATA/ REVERS, FORMESS
      DATA  ((REVERS(I),I=1,91) =
     X-76.330, -74.640, -74.300, -74.170, -72.110, -71.220, -71.120,
     X-69.930, -69.440, -68.840, -68.510, -67.770, -67.100, -66.650,
     X-64.620, -64.140, -63.280, -62.750, -60.530, -60.010, -59.690,
     X-59.430, -58.940, -58.040, -56.660, -55.920, -54.160, -52.410,
     X-49.580, -47.910, -47.260, -46.760, -45.790, -45.320, -45.240,
     X-44.770, -44.690, -44.210, -44.010, -43.640, -43.560, -43.340,
     X-43.260, -42.280, -41.960, -41.520, -41.460, -41.150, -40.970,
     X-40.710, -40.250, -40.030, -40.000, -39.770, -39.470, -39.420,
     X-39.110, -39.030, -38.920, -38.830, -38.770, -38.680, -38.260,
     X-37.890, -37.820, -37.610, -35.000, -34.520, -34.070, -33.610,
     X-33.550, -33.160, -32.170, -31.900, -31.840, -31.500, -30.930,
     X-30.480, -30.420, -29.780, -29.330, -28.520, -28.440, -28.350,
     X-28.030, -27.830, -27.370, -27.050, -26.980, -26.860, -25.430)
      DATA ((REVERS(I),I=92,197) =
     X-25.250, -24.970, -24.820, -24.590, -24.410, -24.070, -23.630,
     X-23.400, -23.290, -23.080, -22.900, -22.69, -22.340, -22.09,
     X-21.79, -21.31, -20.11, -19.80, -19.22, -18.75, -18.72,
     X-18.49, -18.12, -17.47, -17.27, -17.19, -17.00, -16.96,
     X-16.63, -15.57, -15.42, -15.24, -15.13, -14.91, -14.40,
     X-14.28, -13.84, -13.58, -13.30, -13.08, -12.88, -12.65,
     X-12.59, -12.50, -12.46, -12.09, -11.80, -11.66, -11.47,
     X-10.95, -10.88, -10.40, -10.34, -10.21, -9.93, -9.91,
     X-9.61, -9.58, -9.28, -9.27, -8.93, -8.88, -8.71, -8.59,
     X-8.51, -8.37, -8.21, -8.11, -7.69, -7.30, -7.24, -7.17,
     X-6.75, -6.68, -6.59, -6.39, -6.26, -5.94, -5.66, -5.58,
     X-5.18, -4.54, -4.39, -4.35, -4.23, -4.11, -4.01, -3.88,
     X-3.78, -3.32, -3.06, -2.94, -2.90, -2.80, -2.43, -2.13,
     X-2.11, -1.98, -1.95, -1.79, -1.64, -1.63, -1.61, -0.95,
     X-0.89, -0.69)
      DATA ((REVERS(I),I=198,301) =
     X 0.69, 0.89, 0.95, 1.61, 1.63, 1.64, 1.79, 1.95, 1.98,
     X 2.11, 2.13, 2.43, 2.80, 2.90, 2.94, 3.06, 3.32, 3.78,
     X 3.88, 4.01, 4.11, 4.23, 4.35, 4.39, 4.54, 5.18, 5.58,
     X 5.66, 5.94, 6.26, 6.39, 6.59, 6.68, 6.75, 7.17, 7.24,
     X 7.30,7.69,8.11,8.21,8.37,8.51,8.59,8.71,8.88,8.93,
     X 9.27, 9.28, 9.58, 9.61, 9.91, 9.93, 10.21, 10.34, 10.40,
     X 10.88, 10.95, 11.47, 11.66, 11.80, 12.09, 12.46, 12.50,
     X 12.59, 12.65, 12.88, 13.08, 13.30, 13.58, 13.84, 14.28,
     X 14.40, 14.91, 15.13, 15.24, 15.42, 15.57, 16.63, 16.96,
     X 17.00, 17.19, 17.27, 17.47, 18.12, 18.49, 18.72, 18.75,
     X 19.22, 19.80, 20.11, 21.31, 21.79, 22.09, 22.34, 22.69,
     X 22.90, 23.08, 23.29, 23.40, 23.63, 24.07, 24.41, 24.59,
     X 24.82)
      DATA ((REVERS(I),I=302,394) =
     X 24.970,  25.250,  25.430,  26.860,  26.980,  27.050,  27.370,
     X 27.830,  28.030,  28.350,  28.440,  28.520,  29.330,  29.780,
     X 30.420,  30.480,  30.930,  31.500,  31.840,  31.900,  32.170,
     X 33.160,  33.550,  33.610,  34.070,  34.520,  35.000,  37.610,
     X 37.820,  37.890,  38.260,  38.680,  38.770,  38.830,  38.920,
     X 39.030,  39.110,  39.420,  39.470,  39.770,  40.000,  40.030,
     X 40.250,  40.710,  40.970,  41.150,  41.460,  41.520,  41.960,
     X 42.280,  43.260,  43.340,  43.560,  43.640,  44.010,  44.210,
     X 44.690,  44.770,  45.240,  45.320,  45.790,  46.760,  47.260,
     X 47.910,  49.580,  52.410,  54.160,  55.920,  56.660,  58.040,
     X 58.940,  59.430,  59.690,  60.010,  60.530,  62.750,  63.280,
     X 64.140,  64.620,  66.650,  67.100,  67.770,  68.510,  68.840,
     X 69.440,  69.930,  71.120,  71.220,  72.110,  74.170,  74.300,
     X 74.640,  76.330)
```

```
      DATA (FORMESS = 8HRAPIDOGR, 8HAPH PEN , 8HMEDIUM  )
      DIMENSION REVERS (394), XX(394), ANAME(10), AKM(3), FORMESS(3)
      COMMON T(7000)
      REAL LEDGE, MX, MZ, MAXRATE
      INTEGER  SIGN, PUP, PDOWN, PSUP, PSDOWN, PLOTEND
      DTOR = 0.0174533
      JCNTR = 1
      PUP = 3
      PDOWN = 2
      PSUP = -1
      PSDOWN = -2
      PLOTEND = -3
      AKM(2) = 8H KM PER
      AKM(3) = 8HINCH
      M = N = 394
      CALL UNEQUIP (10)
      CALL EQUIP (10, 8HPLOT    )
      CALL DATE (ANAME(9))
      CALL ARMYTIME (ANAME(10))
      WRITE (61,122) ANAME(9), ANAME(10)
  122 FORMAT ('0THEOMAG  ',2A8)
      WRITE (61,119)
  119 FORMAT ('0ALL NUMERICAL INPUT MUST HAVE A DECIMAL POINT'/,
     1        '0SPREADING PARAMETERS')
   10 WRITE (61,100)
  100 FORMAT ('0GIVE THE LEFT EDGE IN MILLION YEARS')
      READ (60,101) LEDGE
  101 FORMAT (F10.0)
      IF (LEDGE .GT. -76.33 .AND. LEDGE .LT. +76.) GO TO 20
      WRITE (61,102)
  102 FORMAT ('-LEFT EDGE IN ERROR')
      GO TO 10
   20 WRITE (61,103)
  103 FORMAT ('0GIVE THE RIGHT EDGE IN MILLION YEARS')
      READ (60,101) REDGE
      IF (REDGE .GT. LEDGE .AND. REDGE .LT. +76.33) GO TO 30
      WRITE (61,104)
  104 FORMAT ('-RIGHT EDGE IN ERROR')
      GO TO 10
C   SET LEDGE EQUAL TO A REVERS BOUNDARY -- CHOSE A
C   LEDGE <= LEDGE
   30 DO 40 I = 2,N
      K = I
      IF (LEDGE .GT. REVERS (I)) GO TO 40
      IF (LEDGE .LT. REVERS (I)) K = K - 1
      LEDGE = REVERS (K)
      ISLEDGE = K
      GO TO 42
   40 CONTINUE
C   REDGE MUST EQUAL A REVERS BOUNDARY -- CHOSE A REDGE >= REDGE
   42 N = K
      L = N + 1
      DO 50 I = L,M
      K = I
      IF (REDGE .GT. REVERS (I)) GO TO 50
      REDGE = REVERS (I)
      GO TO 52
   50 CONTINUE
   52 M = K
C   LEDGE = REVERS (N)      AND     REDGE = REVERS (M)
      J = 1
```

```
      XX(1) = 0.0
C   THE NEXT TWO VARIABLES ARE THE LEFT AND RIGHT INDEXES FOR
C   THE MODEL
      ILEDGE = M
      IREDGE = M
      ISRB1 = ILEDGE
C   SRB1 IS THE LEFT SPREADING RATE BOUNDARY
C   SRB1 = REVERS (ISRB1)
      SRB1 = LEDGE
      SRB2 = REDGE
      ISRB2 = IREDGE
      IF (ILEDGE .LT. IREDGE) GO TO 60
      WRITE (61,105)
  105 FORMAT ('-EDGE ERRORS')
      GO TO 10
   60 WRITE (61,106)
  106 FORMAT ('0GIVE THE SPREADING RATE IN CM PER YEAR')
      READ (60,101) SRATE
      IF (SRATE .GT. 0. .AND. SRATE .LT. 20.) GO TO 70
      WRITE (61,107)
  107 FORMAT ('-SPREADING RATE ERROR')
      GO TO 60
   70 IF (SRATE .GT. MAXRATE) MAXRATE = SRATE
      WRITE (61,108)
  108 FORMAT ('0ANOTHER SPREADING RATE? -- YES OR NO.')
      READ (60,109) IANS
  109 FORMAT (A4)
      IF (IANS .EQ. 4HNO  ) GO TO 90
      IF (IANS .EQ. 4HYES ) GO TO 80
      WRITE (61,110)
  110 FORMAT ('-ILLEGABLE RESPONCE -- TRY AGAIN')
      GO TO 70
   80 WRITE (61,111)
  111 FORMAT ('0GIVE THE RIGHT BOUNDARY OF THE SPREADING RATE IN '/
     1        ' MILLION YEARS')
      READ (60,101) SRB2
      IF (LEDGE .LT. SRB2 .AND. SRB2 .LE. REDGE) GO TO 85
      WRITE (61,112)
  112 FORMAT ('-RIGHT SPREADING RATE BOUNDARY IN ERROR')
      GO TO 80
   85 DO 87 I = ILEDGE, IREDGE
      K = I
      IF (SRB2 .EQ. REVERS (I)) GO TO 88
   87 CONTINUE
      WRITE (61,130)
  130 FORMAT ('-RIGHT SPREADING RATE BOUNDARY NOT A REVERSAL BOUNDARY')
      GO TO 80
   88 ISRB2 = K
C   NOW GENERATE MODEL FROM SRB1 TO SRB2 IE. REVERS(ILEDGE) TO REVERS(IREDGE)
C   CAREFUL  J'S ARE 1 TOO BIG SUCH THAT XX(0) IS XX(1)
   90 ISRB2M1 = ISRB2 - 1
      SRATE = SRATE * 10.
      DO 95 I = ISRB1, ISRB2M1
      J = J + 1
      IF (I .EQ. 183) JCNTR = J
   95 XX(J) = ABS(REVERS (I+1) - REVERS(I)) * SRATE + XX(J-1)
      ISRB1 = ISRB2
      SRB1 = SRB2
      ISRB2 = IREDGE
      SRB2 = REDGE
      IF (ISRB1 .LT. IREDGE) GO TO 60
```

```
C  THE MODEL IS GENERATED  IT GOES FROM 2 TO J
  200 CONTINUE
      WRITE (61,136)
  136 FORMAT ('0GIVE LATITUDE OF THE SPREADING CENTER IN DECIMAL DEGS')
      READ (60,101) SCLAT
      IF (SCLAT .GT. -90. .AND. SCLAT .LT. 90.) GO TO 204
      WRITE (61,137)
  137 FORMAT ('-LATITUDE ERROR')
      GO TO 200
  204 WRITE (61,125)
  125 FORMAT ('0GIVE THE ANGLE BETWEEN POSITIVE X AXIS AND GEOGRAPHIC',/
     1        ' NORTH, MEASURED CLOCKWISE FROM GEOG. N. IN DEGS')
      READ (60,101) THETA
      IF (THETA .GE. 0. .AND. THETA .LE. 360.) GO TO 205
      WRITE (61,131)
      GO TO 204
  205 WRITE (61,138)
  138 FORMAT ('0MODEL AND FIELD PARAMETERS')
      WRITE (61,113)
  113 FORMAT ('0GIVE THE DEPTH TO TOP OF MAGNETIC LAYER IN KM')
      READ (60,101) Z1
      IF (Z1 .GT. 0.0 .AND. Z1 .LT. 15.) GO TO 210
      WRITE (61,114)
  114 FORMAT ('-UPPER BOUNDARY ERROR')
      GO TO 200
  210 WRITE (61,115)
  115 FORMAT ('0GIVE THE DEPTH TO BOTTOM OF MAGNETIC LAYER IN KM')
      READ (60,101) Z2
      IF (Z2 .GT. Z1 .AND. Z2 .LT. 20.) GO TO 220
      WRITE (61,116)
  116 FORMAT ('-LOWER BOUNDARY ERROR')
      GO TO 200
C  WE NOW HAVE MODEL AND Z1 AND Z2
  220 CONTINUE
C  CHECK FOR EDGE EFFECTS
      Z1T40 = 40. * Z1 * MAXRATE / 3.
C  GET THE MAGNETIZATION PARAMETERS
  260 WRITE (61,121)
  121 FORMAT ('0GIVE THE REMANANT MAG IN EMU PER CC ')
      READ (60,101) RM
      RF = RM * 31200. * SQRTF(1. + 3. *(SIN (SCLAT * DTOR) ** 2))
      IF (RF .GT. -5000. .AND. RF .LT. 5000.) GO TO 270
      WRITE (61,131)
  131 FORMAT ('-OUT OF BOUNDS -- TRY AGAIN')
      GO TO 260
  270 RDECL = 0.0
      RINCL = ATAN (2. * TANF (SCLAT * DTOR)) / DTOR
  310 WRITE (61,126)
  126 FORMAT ('0GIVE DECLINATION OF PROFILE CENTER')
      READ (60,101) PDECL
      IF (PDECL .GE. 0. .AND. PDECL .LE. 360.) GO TO 320
      WRITE (61,131)
      GO TO 310
  320 WRITE (61,127)
  127 FORMAT ('0GIVE INCLINATION OF PROFILE CENTER')
      READ (60,101) PINCL
      IF (PINCL .GE. -90. .AND. PINCL .LE. 90.) GO TO 325
      WRITE (61,131)
      GO TO 320
  325 WRITE (61,118) XX(J)
  118 FORMAT ('0THE MODEL IS',F8.1,' KM LONG')
```

```
  222 WRITE (61,120)
  120 FORMAT ('0GIVE THE NUMBER OF FIELD POINTS ')
      READ (60,101) FP
      IFP = FP + .1
      IF (IFP .GT. 0 .AND. IFP .LT. 7000) GO TO 330
      WRITE (61,133)
  133 FORMAT ('-IFP MUST BE LESS THAT 7000')
      GO TO 222
  330 MX = RF * COS (DTOR * RINCL) * COS (DTOR * (THETA - RDECL))
      XINC = XX(J) / IFP
      MZ = RF * SIN (DTOR * RINCL)
      DO 500 K = 1,IFP
C   FIND POINT )= Z0Z1 FROM XX(K) CALL IT IREND
      DO 340 I = 2, J
      M = I
      IF (XX(I) - (K-1) * XINC .GT. Z1T40) GO TO 350
  340 CONTINUE
  350 IREND = M
      IF (IREND .EQ. J) IREND = J - 1
C   FIND POINT (= Z0Z1 FROM XX(K) CALL IT ILEND
      I = IREND
  360 I = I - 1
      IF (I .LE. 2) GO TO 370
      IF ((K-1) * XINC - XX(I) .LT. Z1T40) GO TO 360
  370 ILEND = I
C   THIS LOOP SUMS FOR 1 FIELD POINT
      STP = 0.0
      STN = 0.0
      SL = 1.0
C   THIS LOOP SUMS EFFECTS OF NEIGHBORING BLOCKS FOR A FIELD POINT
      KONST = MOD (ISLEDGE, 2)
      DO 400 I = ILEND, IREND
      XFP = XX(I) - (K-1) * XINC
      SIGN = 1
C   IF (I IS EVEN) SIGN = 1
C   IF (I IS ODD ) SIGN = 0
      IF (MOD(I+KONST,2)) SIGN = 0
      XFPSQ = XFP * XFP
      A = ((Z1 - Z2) / XFP) / (1.0 + ((Z1 * Z2) / XFPSQ))
      IF (XFP .EQ. 0.) A = 0.0
      IF (SIGN) GO TO 380
C   FOR ODD I'S
      STP = (STP+ A) / (1.0 - STP* A)
      GO TO 390
C   FOR EVEN I'S
  380 STN = (STN+ A) / (1.0 - STN* A)
  390 C = (XFPSQ + Z2 * Z2) / (XFPSQ + Z1 * Z1)
      IF (SIGN) C = 1.0 / C
      SL = SL * C
  400 CONTINUE
      P = ATAN2 (STP - STN, 1.0 + STP * STN)
      Q = LOGF (SL) * (-0.5)
C   NOW WE HAVE CALCULATED P AND Q
      V = 4. * (MX * Q - MZ * P)
      H = 4. * (MX * P + MZ * Q)
  500 T(K) = V * SIN (DTOR * PINCL) + H * COS (DTOR * PINCL) *
     1       COS (DTOR * (THETA - PDECL))
C   NOW WE CAN PLOT THE DATA
C   THIS STARTS THE PLOTTING OF THE MODEL
C   COMPUTE THE MAXIMUM ANOMALY FOR SCALING PURPOSES
      TMAX = 0.0
```

```
      DO 590 I = 1,IFP
      IF (ABS(T(I)) .GT. TMAX) TMAX = ABS(T(I))
  590 CONTINUE
      WRITE (61,134) TMAX
  134 FORMAT ('0MAXIMUM ANOMALY IS ',F5.0,' GAMMAS')
C  GET THE VERTICAL SCALE IN GAMMAS PER INCH
  600 WRITE (61,129)
  129 FORMAT ('0GIVE THE VERTICAL SCALE IN GAMMAS PER INCH')
      READ (60,101) VSCALE
      IF (VSCALE .GT. 50. .AND. VSCALE .LT. 500.) GO TO 605
      WRITE (61,132)
  132 FORMAT ('-VERTICAL SCALE IN ERROR')
      GO TO 600
C  CHECK THE PLOT WIDTH FOR THE PAPER SIZE
  605 WIDTH = 2.0 * TMAX / VSCALE + 2.
      IF (WIDTH .LT. 25.) GO TO 610
      WRITE (61,135)
  135 FORMAT ('-PLOT TOO WIDE FOR PAPER')
      GO TO 600
C  GET THE HORIZONAL SCALE IN KM PER INCH
  610 WRITE (61,120)
  120 FORMAT ('0GIVE THE HORIZONAL SCALE IN KM PER INCH')
      READ (60,101) HSCALE
      IF (HSCALE .GE. 1.0 .AND. HSCALE .LE. 150.) GO TO 620
      WRITE (61,142)
  142 FORMAT ('-HORIZONAL SCALE IN ERROR')
      GO TO 610
C  CHECK THE PLOT LENGTH
  620 TLENGTH = XX(J) / HSCALE + 2.
      IF (TLENGTH .GT. 5. .AND. TLENGTH .LT. 60.) GO TO 624
      WRITE (61,123)
  123 FORMAT ('-PLOT LENGTH LONGER THAN 60 INCHES')
      GO TO 610
C  CHECK FOR RAPIDOGRAPH PEN
  624 WRITE (61,117)
  117 FORMAT ('0DO YOU WANT A RAPIDOGRAPH PEN - YES OR NO')
      READ (60,109) IANS
      IF (IANS .EQ. 4HNO  ) GO TO 630
      IF (IANS .EQ. 4HYES ) GO TO 626
      WRITE (61,110)
      GO TO 624
  626 CALL FORMS (10, FORMESS)
C  GET THE USERS NAME SO HE CAN GET THE PLOT BACK
  630 WRITE (61,124)
  124 FORMAT ('0GIVE THE USERS NAME')
      READ (60,139) (ANAME (I),I=1,8)
  139 FORMAT (10A8)
      CALL PLOTINT (-6., 6., 10)
      CALL PLOT (1., 0., PLOTEND)
C  NOW WE HAVE AN ORIGIN 1 INCH FROM THE EDGE OF THE PAPER
C  LABEL THE PLOT WITH USERS NAME, DATE AND TIME
      CALL PLOTSYMB (0., -2., .25, ANAME, 0., 80)
      CALL PLOT (11., 2., PLOTEND)
C  MAKE X AXIS ALONG THE PAPER
      CALL ROTATEXY
C  CALCULATE 1/2 HEIGTH OF VERTICAL AXIS
      FINVA = INVA = TMAX / VSCALE + 1.0
C  GET THE PLOT LABEL
      WRITE (61,143)
  143 FORMAT ('0GIVE THE PLOT LABEL')
      READ (60,139) ANAME
```

```
      CALL PLOTSYMB (0., -FINVA-3., .25, ANAME, 0., 80)
C  CALCULATE MINIMUM VERTICAL SCALE LABEL
      FMAXG = -FINVA * VSCALE
      ENCODE (8, 141, YLAB) FMAXG
  141 FORMAT (F8.0)
C  LABEL MINUMUM VERTICAL SCALE
      CALL PLOTSYMB (-1.5, -FINVA-.10, .15, YLAB, 0., 8)
C  MAKE THE VERTICAL AXIS
      Y = -FINVA
      CALL PLOTSYMB (0., Y, .25, 13, 90., PSUP)
  635 Y = Y + 1
      IF (Y .EQ. 0.) GO TO 635
      IF (Y .GT. FINVA + .5) GO TO 640
      CALL PLOTSYMB (0., Y, .25, 13, 90., PSDOWN)
      GO TO 635
C  CALCULATE MAXIMUM VERTICAL SCALE LABEL
  640 FMAXG = - FMAXG
      ENCODE (8, 141, YLAB) FMAXG
C  AND LABEL MAXIMUM VERTICAL SCALE
      CALL PLOTSYMB (-1.5, FINVA-.10, .15, YLAB, 0., 8)
C  LABEL ZERO ON THE VERTICAL AXIS
      CALL PLOTSYMB (-.75, -.10, .15, 0, 0., 1)
C  IF SPREADING CENTER ON PLOT MARK IT FIRST
      XINIT = 0.0
      CALL PLOT (0., 0., PUP)
      IF (JCNTR .EQ. 1) GO TO 650
      XINIT = X = (XX(JCNTR) + XX(JCNTR -1)) / (HSCALE * 2.)
      CALL PLOTSYMB (X, 0., .35, 13, 0., PSUP)
C  LABEL SPREADING CNTR IF PRESENT
      CALL PLOTSYMB (X, 0.5, .20, 0, 0., 1)
      CALL PLOT (X, 0., PUP)
C  MAKE KM TICKS BACK TO YAXIS
  645 X = X - 1.
      IF (X .LT. 0.) GO TO 650
      CALL PLOTSYMB (X, 0., .25, 13, 0., PSDOWN)
      GO TO 645
C  MAKE KM TICKS FROM SPREADING CNTR TO RIGHT END
  650 CALL PLOT (0., 0., PDOWN)
      X = XINIT
      CALL PLOT (X, 0., PUP)
  655 X = X + 1.
      CALL PLOTSYMB (X, 0., .25, 13, 0., PSDOWN)
      IF (X .GT. XX(J)/HSCALE) GO TO 660
      GO TO 655
C  PUT KM SCALE ON PLOT
  660 ENCODE (8, 144, AKM(1)) HSCALE
  144 FORMAT (F8.2)
      CALL PLOTSYMB (X, 0., .10, AKM, 0., 20)
C  MAKE MODEL BLOCKS
C  SIGN IS -2 FOR POSITIVE BLOCKS
C  SIGN IS -1 FOR NEGATIVE BLOCKS
      Y = -FINVA -1.
      ENCODE (8, 144, AKM(1)) REVERS (ISRB2)
      CALL PLOTSYMB (XX(J)/HSCALE -.5, Y+.5, .10, AKM(1), 0., 8)
      CALL PLOTSYMB (XX(J) / HSCALE, Y, .25, 13, 0., PSUP)
      I = J
      K = ISRB2
  665 I = I - 1
      IF (I .EQ. 0) GO TO 670
      SIGN = -2 + MOD (K,2)
      K = K - 1
```

```
      CALL PLOTSYMB (XX(I) / HSCALE, Y, .25, 13, 0., SIGN)
      GO TO 665
  670 ENCODE (8,144, AKM(1)) REVERS (ISLEDGE)
      CALL PLOTSYMB (XX(1)/HSCALE-.5, Y+.5, .10, AKM(1), 0., 8)
C  FINALLY WE CAN PLOT THE TOTAL FIELD
      X = 0.
      CALL PLOT (X/HSCALE, T(1) / VSCALE, PUP)
      DO 675 I = 2,IFP
      X = X + XINC
  675 CALL PLOT (X/HSCALE, T(I) / VSCALE, PDOWN)
      CALL PLOT (TLENGTH + 6., +15., PLOTEND)
  678 WRITE (61,145)
  145 FORMAT ('0DO YOU WANT TO SAVE THE TOTAL FIELD VALUES')
      READ (60,109) IANS
      IF (IANS .EQ. 4HYES ) GO TO 680
      IF (IANS .EQ. 4HNO  ) GO TO 690
      WRITE (61,110)
      GO TO 678
  680 CALL EQUIP (1,8HFILE    )
      BUFFER OUT (1,1) (T, T(IFP))
      WRITE (61,146)
  146 FORMAT ('0GIVE THE NAME OF THE TOTAL FIELD FILE')
      READ (60,139) FILENAME
      CALL SAVE (1,FILENAME)
  690 CONTINUE
      CALL RESET
      END
```

```
      PROGRAM TWOMAG
C
      DIMENSION HX(2000),HZ(2000),HT(2000),X(2000)
      REAL MI,MD,M,JX,JZ,JXP,JZP
C
C*****************************************************************************
C
C       PROGRAM TWOMAG COMPUTES THE HORIZONTAL, VERTICAL, AND TOTAL FIELD
C    ANOMALY PROFILES PRODUCED BY ONE OR MORE TWO-DIMENSIONAL MAGNETIC
C    BODIES WITH ARBITRARY CROSS-SECTIONAL SHAPE.  ASSUMPTIONS
C    ARE (1) THE BODY IS INFINITELY EXTENDED IN THE PLUS AND
C    MINUS Y DIRECTIONS, (2) EACH BODY IS UNIFORMLY MAGNETIZED,
C    AND (3) EACH BODY CAN BE APPROXIMATED BY A POLYGON.
C       PROGRAM WRITTEN BY RICHARD J. BLAKELY, SCHOOL OF OCEAN-
C    OGRAPHY, OREGON STATE UNIVERSITY, CORVALLIS, OREGON 97331.
C    LAST UPDATE WAS MADE ON SEPTEMBER 16, 1975.
C
C
C   INPUTS -
C
C      EACH RUN REQUIRES THE FOLLOWING DATA ON ONE CARD (FMT 2I5,7F10.1)...
C       NX -      THE NUMBER OF DATA POINTS REQUIRED.
C       IPUNCH -  IF IPUNCH = 1, THE TOTAL FIELD ANOMALY WILL BE PUNCHED
C                 ON CARDS.  IF IPUNCH = 0, NO ACTION.
C       XSTART -  THE STARTING X-COORDINATE (KM).
C       XDELT -   THE SPATIAL SAMPLE INTERVAL (KM).
C       MI -      THE INCLINATION OF THE MAGNETIZATION OF THE SOURCE
C                 (DEGREES).
C       MD -      THE DECLINATION OF THE MAGNETIZATION.
C       FI -      THE INCLINATION OF THE REGIONAL FIELD.
C       FD -      THE DECLINATION OF THE REGIONAL FIELD.
C       TREND -   THE TREND OF THE TWO-DIMENSIONAL SOURCE.
C
C      EACH BODY REQUIRES THE FOLLOWING DATA ON ONE CARD (FMT I5,F10.1)...
C
C       NSIDES - THE NUMBER OF SIDES TO THE PRISM.
C       M -      THE MAGNITUDE OF THE MAGNETIZATION (EMU/CC).
C
C      EACH CORNER OF THE BODY REQUIRES THE FOLLOWING DATA
C      ON ONE CARD (FMT(2F10.1)...
C
C       X2 -      THE X COORDINATE (KM).
C       Z2 -      THE Y COORDINATE.
C
C
C    NOTE 1 - THE COORDINATES OF THE CORNERS SHOULD BE TAKEN CLOCKWISE.
C             FOR EXAMPLE, THE DATA REQUIRED (NSIDES,M,X1,Z1) FOR A
C             UNIT-SQUARE BODY AT 1 KM DEPTH ARE AS FOLLOWS...
C
C     4       .005
C        -.5          .5
C         .5          .5
C         .5         1.5
C        -.5         1.5
C              (BLANK)
C
C    NOTE 2 - ONE BLANK CARD TERMINATES THE PROFILE AND A NEW PROFILE
C             IS INITIATED; TWO BLANK CARDS TERMINATE THE PROGRAM.
C
C    NOTE 3 - THE PARAMETER [TREND] DETERMINES THE DIRECTION OF THE
C             PROFILE TRACK AS FOLLOWS.  [TREND] DETERMINES THE POSITIVE
```

```
C             Y DIRECTION, Z IS POSITIVE DOWNWARD, AND THE X-AXIS IS IN
C             THE SENSE OF A RIGHT HANDED SYSTEM.  THE PROFILE IS TAKEN
C             IN THE POSITIVE X-DIRECTION.
C    NOTE 4 - LOGICAL UNITS ARE... 5 = CARD INPUT
C                                   6 = LINE PRINTER OUTPUT
C                                   7 = CARD PUNCH.
C    NOTE 5 - IN SUBROUTINE RIBBON, A FUNCTION CALLED ARCTAN IS
C             USED WHICH IS DIFFERENT THAN THE STANDARD
C             FUNCTION ATAN2.  ARCTAN(X,Y) IS DEFINED AS
C             ARCTAN(Y/X) AND IS EQUIVALENT TO ATAN2(Y,X).
C
C*************************************************************************
C
      WRITE(6,100)
  100 FORMAT(1H1)
 1002 READ(5,100)NX,IPUNCH,XSTART,XDELT,MI,MD,FI,FD,TREND
  100 FORMAT(2I5,7F10.1)
      IF(NX.EQ.0)GO TO 1003
      KLAB=0
      WRITE(6,102)NX,IPUNCH,XSTART,XDELT,MI,MD,FI,FD,TREND
  102 FORMAT(///,' INPUT TO TWOMAG...',//,10X,'NX = ',I5,/,10X,'IPUNCH =
     1 ',I5,/,10X,'XSTART = ',F10.1,/,10X,'XDELT = ',F10.1,/,10X,'MI = '
     2,F10.1,/,10X,'MD = ',F10.1,/,10X,'FI = ',F10.1,/,10X,'FD = ',F10.1
     3,/,10X,'TREND = ',F10.1////)
      CONV=3.14159/180.
      MI=MI*CONV
      MD=MD*CONV
      FI=FI*CONV
      FD=FD*CONV
      TREND=TREND*CONV
      JXP=-COS(MI)*SIN(MD-TREND)
      JZP=SIN(MI)
      A=-COS(FI)*SIN(FD-TREND)
      B=SIN(FI)
      DO 1 I=1,NX
      HX(I)=HZ(I)=HT(I)=0.
    1 X(I)=XSTART+XDELT*FLOAT(I-1)
 1000 READ(5,106)NSIDES,M
  106 FORMAT(I5,F10.1)
      IF(NSIDES.EQ.0)GO TO 1001
      KLAB=KLAB+1
      WRITE(6,107)KLAB,M
  107 FORMAT('    BLOCK NUMBER ',I5,'      M = ',E10.3,//,8X,'X1',8X,'Z1',
     1//)
      JX=JXP*M
      JZ=JZP*M
      NT=NSIDES+1
      DO 2 J=1,NT
      IF(J.NE.1)GO TO 6
      READ(5,101)X2,Z2
      WRITE(6,101)X2,Z2
  101 FORMAT(2F10.1)
      XT=X2
      ZT=Z2
      GO TO 2
    6 CONTINUE
      IF(J.NE.NT)GO TO 7
      X1=X2
      Z1=Z2
      X2=XT
      Z2=ZT
```

```
      GO TO 8
    7 CONTINUE
      X1=X2
      Z1=Z2
      READ(5,101)X2,Z2
      WRITE(6,101)X2,Z2
    8 CONTINUE
      DO 3 I=1,NX
      CALL RIBBON(X(I),0.,X1,Z1,X2,Z2,JX,JZ,FX,FZ)
      FT=A*FX+B*FZ
      HX(I)=HX(I)+FX
      HZ(I)=HZ(I)+FZ
    3 HT(I)=HT(I)+FT
    2 CONTINUE
      GO TO 1000
 1001 WRITE(6,103)
  103 FORMAT(//,'  RESULTS OF TWOMAG',//,3X,'STATION',2X,'LOCATION',9X,
     1'X',9X,'Z',5X,'TOTAL'/)
      DO 5 I=1,NX
    5 HT(I)=HT(I)*10.**5
      WRITE(6,104)(I,X(I),HX(I),HZ(I),HT(I),I=1,NX)
  104 FORMAT(I10,4E10.3)
      IF(IPUNCH.NE.1)GO TO 4
      WRITE(7,105)(HT(I),I=1,NX)
  105 FORMAT(8F8.0)
    4 CONTINUE
      GO TO 1002
 1003 STOP
      END
      SUBROUTINE RIBBON(X0,Z0,X1,Z1,X2,Z2,JX,JZ,FX,FZ)
      REAL JX,JZ
C
C     SUBROUTINE RIBBON COMPUTES THE X AND Z COMPONENTS (FX,FZ) AT SOME
C   POINT (X0,Z0) DUE TO A RIBBON INFINITE IN THE Y-DIRECTION AND
C   BOUNDED IN THE X-Z PLANE BY (X1,Z1) AND (X2,Z2).  THE MOMENT OF THE
C   RIBBON IS DETERMINED BY THE MAGNETIZATION VECTOR (JX,JZ) , THE MAG-
C   NETIC MEDIA BEING CLOCKWISE TO THE VECTOR FROM (X1,Z1) TO (X2,Z2).
C
      SX=X2-X1
      SZ=Z2-Z1
      S=SQRT(SX**2+SZ**2)
      SX=SX/S
      SZ=SZ/S
C
      QS=JX*SZ-JZ*SX
C
      R1X=X1-X0
      R1Z=Z1-Z0
      R2X=X2-X0
      R2Z=Z2-Z0
      R1=SQRT(R1X**2+R1Z**2)
      R2=SQRT(R2X**2+R2Z**2)
C
      T1=ARCTAN(R1X,R1Z)
      T2=ARCTAN(R2X,R2Z)
C
      FS=2.*QS*ALOG(R1/R2)
      FN=2.*QS*(T1-T2)
C
      FX=FN*SZ+FS*SX
      FZ=-FN*SX+FS*SZ
      RETURN
      END
```

```
      PROGRAM WAREFRA
C THIS PROGRAM COMPUTES PLANE DIPPING LAYER MODEL
C PARAMETERS,SECTIONS OF LAYERS ALONG WHICH RAY IS REFRACTED
C AND THE CRITICAL DISTANCE.  THE INPUT DATA REQUIRES
C KNOWN OR APPARENT LAYER VELICITIES (VA) AND EITHER
C INTERCEPT TIME FROM REFRACTED ARRIVAL OR LAYER THICKNESS
C VERTICALLY UNDER THE ORIGIN. LAYER DIP IS ASSUMED ZERO
C IF LEFT BLANK.  IF LAYER THICKNESS IS GIVEN, GIVEN
C VELOCITY IS TAKEN TO BE THE TRUE LAYER VELOCITY.
      DIMENSION V(10),HDR(10),W(10),VA(10),TIA(10),HA(10)
      DIMENSION  B (10), ALPHA (10), BETA (10), HB (10), A (10)
      DIMENSION XA(10),XB(10),YA(10),YB(10),XC(10),P(10)
      DIMENSION  Q (10)
      RTOD = 180. / 3.14159265
      DTOR = 1. / RTOD
C  READ HDR CARD
   10 READ (5, 100) N, V(1), X, HDR
      IF(EOF(5)) CALL EXIT
C N IS NUMBER OF LAYERS, V(1) IS VELOCITY OF FIRST LAYER,
C X IS LENGTH OF LINE, HDR IS IDENTIFIER MAX LENGTH OF 8
  100 FORMAT (I5,2F5.0,10A8)
      IF (EOF (1)) CALL EXIT
      IF (N .LT. 10) GO TO 15
      WRITE (61, 110) N
  110 FORMAT ('-N LARGER THAN DIMENSIONS  N =',I5)
      CALL EXIT
   15 K = 2
      VA (1) = V (1)
      W (1) = 0.0
C  READ SUCCEEDING CARDS
C IF HA(I)IS NOT GIVEN, COMPUTE MODEL FROM TIA INTERCEPT
      READ (5, 101) VA (2), TIA (2), W (2), HA (1)
  101 FORMAT (4F5.0)
      W (2) = W (2) * DTOR
      BETA (1) = ASINF (V (1) / VA (2))
      A (1) = B (1) = BETA (1) + W (2)
      ALPHA (1) = A (1) + W (2)
      V (2) = V (1) / SIN (A (1))
      IF(HA(1).NE.0.0) V(2)=VA(2)
C  FIND OUT IF THICKNESS GIVEN. IF NOT, CALCULATE VELOCITY AND
C ANGLES.
      IF (HA (1) .NE. 0.0) GO TO 30
      IF (TIA (2) .NE. 0.0) GO TO 25
   22 WRITE (61, 111)
  111 FORMAT ('-HA AND TIA .EQ. 0.0')
      CALL EXIT
C COMPUTE DEPTHS TO LAYERS
   25 HA(1)=(TIA(2)*V(1))/(COS(ALPHA(1))+COS(BETA(1)))
   30 HB (1) = HA (1) - X * TANF(W (2))
C COMPUTE CRITICAL DISTANCES AND END POINTS IN LAYER
C WHERE RAY TRAVELS AS REFRACTED WAVE
      XA (1) = HA (1) * TANF(ALPHA (1))
     1          / (1.0 + TANF(W (2)) * TANF(ALPHA (1)))
      YA (1) = HA (1) - XA (1) * TANF(W (2))
      XC(1)=(HA(1)-XA(1)*TANF(W(2)))*TANF(B(1))+XA(1)
      XB (1) = HB (1) * TANF(BETA (1))
     1          / (1.0 - TANF(BETA (1)) * TANF(W (2)))
      YB (1) = HB (1) + XB (1) * TANF(W (2))
      XB (1) = X - XB (1)
   40 K = K + 1
C DO LAYERS 3 THROUGH N
```

```
      READ (5, 101) VA (K), TIA (K), W (K), HA (K-1)
C COMPUTE ANGLES
      W (K) = W (K) * DTOR
      BETA (1) = ASINF (V (1) / VA (K))
      B (1) = BETA (1) + W (2)
      I = 1
      KM1 = K - 1
   50 I = I + 1
      Q (I) = ASINF (V (I) / V (I-1) * SIN (B (I-1)))
      BETA (I) = Q (I) - W (I)
      B (I) = BETA (I) + W (I+1)
      IF (I .LT. KM1) GO TO 50
      A (K-1) = B (K-1)
      ALPHA (K-1) = A (K-1) + W (K)
      V (K) = V (K-1) / SIN (A (K-1))
      IF(HA(K-1).NE.0.0) V(K)=VA(K)
      P (K-1) = A (K-1) - W (K-1) + W (K)
      I = K - 1
   70 I = I - 1
      A (I) = ASINF (V (I) / V (I+1) * SIN (P (I+1)))
      ALPHA (I) = A (I) + W (I+1)
      P (I) = A (I) - W (I) + W (I+1)
      IF (I .NE. 1) GO TO 70
      KM2 = K - 2
      TEMP1 = TEMP2 = TEMP3 = 0.0
      DO 80 I = 1, KM2
      TEMP1 = TEMP1 + HA (I) / V (I) * (COS (ALPHA (I))
     1          + COS (BETA (I)))
      TEMP2 = TEMP2 + HA (I)
      TEMP3 = TEMP3 + HB (I)
   80 CONTINUE
      IF (HA (K-1) .NE. 0.0) GO TO 85
C FIND OUT IF THICKNESS GIVEN, IF NOT COMPUTE VELOCITY AND
C MORE ANGLES
      IF (TIA (K) .EQ. 0.0) GO TO 22
C COMPUTE DEPTH TO LAYER
      HA (K-1) = (TIA (K) - TEMP1) * V (K-1)
     1           / (COS (ALPHA (K-1)) + COS (BETA (K-1)))
C COMPUTE DISTANCES IN LAYER WHERE WAVE IS REFRACTED
   85 TEMP2 = TEMP2 + HA (K-1)
      HB (K-1) = TEMP2 - TEMP3 - X * TANF(W (K))
      TEMP 3 = TEMP 3 + HB (K-1)
      TEMPXA = HA (1) * TANF(ALPHA (1))
     1          / (1.0 + TANF(W (2)) * TANF(ALPHA (1)))
      TEMPXB = HB (1) * TANF(BETA (1))
     1         / (1.0 - TANF(W (2)) * TANF(BETA (1)))
      DO 115 I = 2, KM1
      TEMPXA = TEMPXA + (HA (I) * TANF(ALPHA (I)) + TEMPXA
     1        * TANF(ALPHA (I)) * (TANF(W (I)) - TANF(W (I+1))))
     2        / (1.0 + TANF(ALPHA (I)) * TANF(W (I+1)))
      TEMPXB = TEMPXB + (HB (I) * TANF(BETA (I))  - TEMPXB
     1        * TANF(BETA (I)) * (TANF(W (I)) - TANF(W (I+1))))
     2        / (1.0 - TANF(BETA (I)) * TANF(W (I+1)))
  115 CONTINUE
      XA (K-1) = TEMPXA
      XB (K-1) = X - TEMPXB
      YA (K-1) = TEMP2 - XA (K-1) * TANF(W (K))
      YB (K-1) = TEMP3 + TEMPXB * TANF(W (K))
      I = K
      DELTAXC = TEMPXA
  120 I = I - 1
```

```
      DELTAXC = DELTAXC + (HA (I) * TANF(BETA (I)) + DELTAXC
     1         * TANF(BETA (I)) * (TANF(W(I)) - TANF(W (I+1))))
     2         / (1.0 - TANF(W (I)) * TANF(BETA (I)))
      IF (I .GT. 2) GO TO 120
      XC (K-1) = DELTAXC + (HA (1) - DELTAXC * TANF(W (2)))
     1          * TANF(BETA (1))
C GO BACK FOR ANOTHER LAYER
      IF (K .LT. N) GO TO 40
C CONVERT ANGLES TO DEGREES
      DO 130 I = 1,N
      W (I) = W (I) * RTOD
  130 CONTINUE
C PRINT OUT RESULTS
      WRITE (61, 102) HDR, N, X
  102 FORMAT ('0',10A8,/,' N = ',I2,'   SPREAD = ',F6.1)
      WRITE (61, 103)
  103 FORMAT ('0 N  APPARENT   DIP   LAYER THICKNESS',/,
     1        '     VELOCITY            AT ORIGIN')
      NM1 = N - 1
      DO 140 I = 1, NM1
      WRITE (61, 104) I, VA (I), W (I), HA (I)
  104 FORMAT (I3,F9.3,F8.3,6X,F6.3)
  140 CONTINUE
      WRITE (61, 104) N, VA (N), W (N)
      WRITE (61, 105)
  105 FORMAT ('0 N  DEPTH A  THICK A  VELOCITY  THICK B  '
     1   'DEPTH B')
      SHA = 0.0
      SHB = 0.0
      DO 150 I = 1, NM1
      SHA = SHA + HA (I)
      SHB = SHB + HB (I)
      WRITE (61, 106) I, SHA, HA (I), V (I), HB (I), SHB
  106 FORMAT (I3,F8.3,F9.3,F10.3,F10.3,F9.3)
  150 CONTINUE
      WRITE (61, 107) N, V (N)
  107 FORMAT (I3,18X,F8.2)
      WRITE (61, 108) X
  108 FORMAT ('0LAYER  RAY TO LAYER  CRITICAL DIST  RAY FROM ',
     1'LAYER',/,'          X      Y                      X',
     2'       Y',/,'       0.00     0.00                  ',
     3 F7.2,'    0.00')
      DO 160 I = 1, NM1
      IP1 = I + 1
      WRITE (61, 109) I, XA (I), YA (I), XC (I), XB (I), YB (I)
  109 FORMAT (I3,F9.3,F8.3,F11.3,F14.3,F8.3)
  160 CONTINUE
      GO TO 10
      END
```